SANDIA REPORT

SAND2005-6846
Unlimited Release
Printed November 2005

Characterization, Performance and Optimization of PVDF as a Piezoelectric Film for Advanced Space Mirror Concepts

Tim R. Dargaville, Mathias C. Celina, Julie M. Elliott, Pavel M. Chaplya, Gary D. Jones, Daniel M. Mowery, Roger A. Assink, Roger L. Clough, Jeffrey W. Martin

Prepared by
Sandia National Laboratories
Albuquerque, New Mexico 87185 and Livermore, California 94550

Sandia is a multiprogram laboratory operated by Sandia Corporation,
a Lockheed Martin Company, for the United States Department of Energy's
National Nuclear Security Administration under Contract DE-AC04-94AL85000.

Issued by Sandia National Laboratories, operated for the United States Department of Energy by Sandia Corporation.

Available to DOE and DOE contractors from
U.S. Department of Energy
Office of Scientific and Technical Information
P.O. Box 62
Oak Ridge, TN 37831

Telephone: (865)576-8401
Facsimile: (865)576-5728
E-Mail: reports@adonis.osti.gov
Online ordering: http://www.osti.gov/bridge

Available to the public from
U.S. Department of Commerce
National Technical Information Service
5285 Port Royal Rd
Springfield, VA 22161

Telephone: (800)553-6847
Facsimile: (703)605-6900
E-Mail: orders@ntis.fedworld.gov
Online order: http://www.ntis.gov/help/ordermethods.asp?loc=7-4-0#online

SAND2005-6846
Unlimited Release
Printed November 2005

Characterization, Performance and Optimization of PVDF as a Piezoelectric Film for Advanced Space Mirror Concepts

Tim Dargaville, Mathew Celina, Julie Elliott, Daniel Mowery, Roger Assink, Roger Clough
Organic Materials

Pavel M. Chaplya
Materials Mechanics

Gary D. Jones
Microsystem Materials

Jeffrey W. Martin
Mechanical Systems Design

Sandia National Laboratories
P.O. Box 5800
Albuquerque, NM 87185-1411

Abstract

Piezoelectric polymers based on polyvinylidene fluoride (PVDF) are of interest for large aperture space-based telescopes as adaptive or smart materials. Dimensional adjustments of adaptive polymer films depend on controlled charge deposition. Predicting their long-term performance requires a detailed understanding of the piezoelectric material features, expected to suffer due to space environmental degradation. Hence, the degradation and performance of PVDF and its copolymers under various stress environments expected in low Earth orbit has been reviewed and investigated. Various experiments were conducted to expose these polymers to elevated temperature, vacuum UV, γ-radiation and atomic oxygen. The resulting degradative processes were evaluated. The overall materials performance is governed by a combination of chemical and physical degradation processes. Molecular changes are primarily induced via radiative damage, and physical damage from temperature and atomic oxygen exposure is evident as depoling, loss of orientation and surface erosion. The effects of combined vacuum UV radiation and atomic oxygen resulted in expected surface erosion and pitting rates that determine the lifetime of thin films. Interestingly, the piezo responsiveness in the underlying bulk material remained largely unchanged. This study has delivered a comprehensive framework for material properties and degradation sensitivities with variations in individual polymer performances clearly apparent. The results provide guidance for material selection, qualification, optimization strategies, feedback for manufacturing and processing, or alternative materials. Further material qualification should be conducted via experiments under actual space conditions.

Acknowledgements
The authors express their appreciation to Bruce Tuttle for use of equipment to measure the d_{33} coefficients, Jonathan Campbell for use of the evaporation chamber, Mark Stavig for DMA measurements, Gary Zender for acquiring the SEM images, Ralph Tissot for the XRD measurements, Ed Stretanski, Mary Rice, Larry Lee and Jim Puissant at Ktech, Garrett Poe at SRS Technologies, Gary Pippin at Boeing, and Bruce Banks, Deborah Waters and Joyce Dever at NASA GRC.

Contents

Figures

Tables

Nomenclature and Abbreviations

AO	=	atomic oxygen
CTFE	=	chlorotrifluoroethylene
d_{33}	=	piezoelectric strain coefficient in the thickness direction
DMA	=	dynamic mechanical analysis
DMAc	=	dimethyl acetamide
DSC	=	differential scanning calorimetry
HFP	=	hexafluoropropylene
HST	=	Hubble Space Telescope
ISS	=	International Space Station
LDEF	=	Long Duration Exposure Facility
LEO	=	low Earth orbit
MISSE	=	Materials International Space Station Experiment
NMR	=	nuclear magnetic resonance
NMP	=	N-methyl-2-pyrrolidinone
PVDF	=	poly(vinylidene fluoride)
P_r	=	remanent polarization
SEM	=	scanning electron microscopy
TrFE	=	trifluoroethylene
T_c	=	Curie transition
T_g	=	glass transition
T_m	=	melting temperature
VUV	=	vacuum ultraviolet
XRD	=	X-ray diffraction

1. Introduction

Major steps in space exploration and utilization can only be achieved via far reaching enabling technologies that employ radically new approaches and engineering solutions to complex problems [1]. For many countries space access and utilization is intrinsically linked to national interests and security considerations resulting in the application of leading edge technologies and long-term strategic research directions. The development of more advanced materials is often one of the driving forces behind innovation in this area. An example is the development and potential use of responsive, smart or adaptive materials based on polymers in space applications representing a critical enabling technology for the 21st century.

Large diameter PVDF film-based adaptive optics have been identified as a promising alternative to overcome weight limitations in high-resolution spaced-based telescope systems similar to the James Web Space Telescope. The challenge in designing novel large-aperture adaptive optics systems providing improved sensitivity and ground resolution for future space-based remote sensing systems is to identify suitable high performance thin film polymeric materials. The shape control in adaptive optics utilizes the responsiveness of piezoelectric polymers such as polyvinylidene fluoride (PVDF) to directed charge deposition. Besides developing charge deposition control feedback loops and addressing engineering design issues [2], a detailed understanding of PVDF material changes and performance when exposed to vacuum UV irradiation, thermal cycling, atomic oxygen and other environmental factors in low Earth orbit space environments is absolutely critical. Materials performance will depend on primary polymer properties, copolymer type, film processing, molecular orientation, morphology and the applied poling technologies (piezoelectric optimization), as well as relative sensitivities to the various conditions in the space environment. There is no commercial optimized material available for such an application. This study aims to investigate the important features of various PVDF-based copolymers, and the accelerated degradation of these polymers to understand how piezoelectric performance limitations depend on molecular structure, morphology and synergistic damage accumulation during radiation, temperature and atomic oxygen exposures. Achieving this goal of material qualification and lifetime prediction has been addressed by a three-year effort with a multidisciplinary team combining Sandia's expertise in polymer materials characterization and degradation with the satellite group's adaptive optics research experience. This LDRD polymer aging and performance research effort was primarily carried out within Dept. 1821.

Piezoelectric polymer films based on PVDF will respond to charge deposition and represent an attractive group of materials for adaptive optics applications. The recent success in wireless shape control methods has demonstrated the feasibility of this technology [2]. Any electron gun control approach for charge deposition requires a detailed understanding of the piezoelectric material responses. Space applications also demand consistent, predictable, and reliable performance. While PVDF (as a generic material class covering various copolymers) so far has been identified as the best material for electrical control purposes, it is also well known that fluorinated polymers are the most sensitive polymers to high-energy radiation. Mechanical properties will suffer with various types of radiation (vacuum UV, γ-, X-ray, charged particles) and extreme temperature fluctuations. Experiments carried out on the low Earth orbit (LEO) long-duration exposure facility (LDEF) in the late 1980's [3-5] and NASA's experience with material selection for both satellite and space station applications, as well as performance feedback from the Hubble space telescope (HST) [6-8] have revealed considerable polymer weaknesses in these environments. While the radiation degradation of polymers is an established field [9] there is little information available on the performance of specialized features such as the piezoelectric and/or similar properties of PVDF with respect to their expected changes upon LEO exposure. Understanding such fundamental issues becomes mandatory for the design and deployment of satellite systems utilizing these materials and technology. Traditional polymer aging studies mostly focus on understanding the chemical

and bulk physical property changes with the emphasis on degradation mechanism and their relevance to lifetime prediction methods. Based on existing literature, the precise details of piezoelectric properties are not even fully established in terms of their dependence on morphology, poling, and crystalline features. The need to fully understand the piezoelectric performance of these polymers under complex LEO environments is a challenging task that has not been addressed by industry. This study examines the many problems facing the polymer material scientist when dealing with the identification and optimization of suitable materials for these applications. It is intended to demonstrate important polymer property variations and the key issues that relate to performance considerations.

As for any other materials application in space environments, a comprehensive understanding of the critical LEO conditions leading to PVDF homo and copolymer performance limitations is required. LEO environmental conditions are highly complex and often synergistic, as well as orbit dependent, so that specific conditions are difficult to predict. Probably the first systematic scientific studies on LEO exposure on polymers and composite materials were conducted as part of the LDEF in the 1980's. They revealed unexpected performance limitations of many materials and demonstrated the complex nature of LEO exposure, synergistic degradation pathways, and associated lifetime prediction [3-5]. The synergistic nature of vacuum UV and atomic oxygen exposure for example was subsequently demonstrated [10,11]. Based on such experimental data, guidance on expected vacuum UV, other energetic radiation and atomic oxygen levels has been provided in a range of NASA publications [12-14]. These discuss actual cumulative environments, as well as experiences with materials performance. Many data have been incorporated and made available in the NASA Materials Selector Expert System database [15]. This database contains information collected on polymer performance and observed damage accumulation originating from many different space missions. The database is intended to provide predictive feedback and allows modeling of expected UV doses, atomic oxygen and other damage parameters under various orbital conditions. However, there are currently no references or data available on anticipated piezoelectric changes or related degradation for PVDF-based polymers in space environments. For the Hubble space telescope in LEO orbit, significant cracking of the outer layer Teflon fluorinated ethylene propylene (FEP) multi-layer insulation was observed during the second servicing mission after 6.8 years in orbit [6,7]. To better understand the failure mechanism and allow for estimated exposure levels through to the mission end-of-life, a full assessment of environmental conditions and various exposure levels was conducted as part of that study [7]. Environmental exposure was primarily seen as a combination of thermal cycling (from -200 °C in the shadow, up to +200 °C in extreme situations), solar UV and X-ray radiation, trapped electron and proton radiation, and exposure to plasma and atomic oxygen. Often it was concluded that individual exposure components alone could not explain the observed failure, putting the emphasis again on complex synergistic environments. It is interesting to note that in this study there was a distinction between direct solar light and atmospherically reflected light for the solar UV exposures and an assessment of total equivalent sun hours for different positions on the spacecraft [7]. Yet, there was no discussion of specific material sensitivities in certain wavelength regions, estimated UV doses required to induce significant changes, vacuum UV degradation pathways and their exposure time dependencies. In general, there seems to be lack of knowledge in the literature on vacuum UV polymer material absorptivities, degradation mechanisms and failure doses. It would appear that one of the key questions in LEO UV exposure, the correlation of total doses and thus total sun hours with material radiation sensitivities and degradative changes, needs further investigation for meaningful LEO life time predictions. This study incorporates some attempts in this direction and as discussed below, expected vacuum UV exposures and material sensitivities are assessed on the basis of highly energetic radiation doses for correlation with screening studies of accelerated γ-irradiation experiments. This study aims to evaluate the full range of available PVDF copolymer materials, determine their respective properties and provide guidance on a multitude of performance criteria, all relevant to final material selection. The schematic diagram below (Fig. 1) demonstrates this complex task of matching a range of available materials and properties with critical performance requirements.

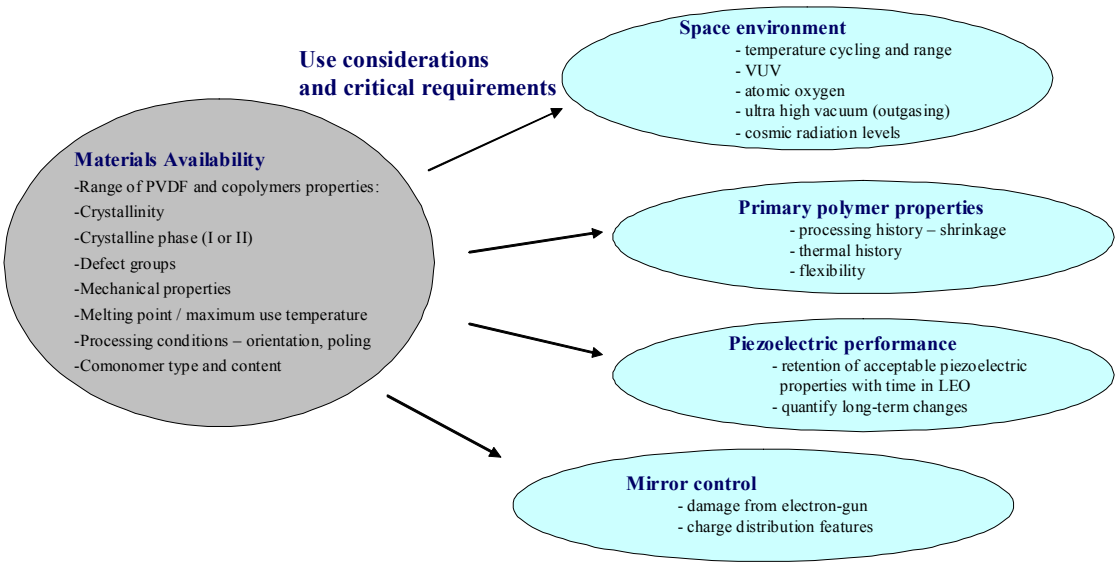

Figure 1. Complex material selection and characterization issues

2. Overview: PVDF based polymers for piezoelectric applications

Polyvinylidene fluoride (PVDF) is a semi-crystalline polymer commercially available as powder, pellets or semi-transparent films (ranging from 8 to 110 μm in thickness). PVDF has a melting temperature of approximately 170 °C and has reasonable melt viscosity suitable for melt processing without the need for processing aids, stabilizers or additives. The polymer can also be solution processed due to its solubility in common polar solvents (NMP, DMAc for example). The glass transition temperature is typically around -40 °C so that at room temperature the polymer is flexible with good mechanical properties. Non-piezoelectric PVDF has many uses in coatings, cable insulation, gaskets, flexible tubing, and parts for handling radioactive materials, to name just a few examples [16]. PVDF is synthesized by addition polymerization of the CH_2=CF_2 monomer. When produced as the homopolymer (i.e. from 100% CH_2=CF_2 monomer), the majority of the PVDF chains have a regular structure of alternating CH_2 and CF_2 groups:

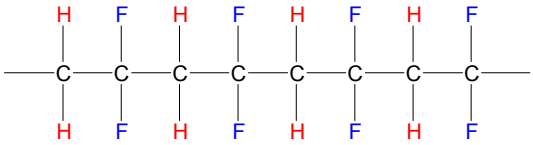

The polymerization, however, is not completely regiospecific, so that the polymer contains occasional reversed monomer units (head-to-head and tail-to-tail) in the otherwise completely head-to-tail sequence (by definition the CF_2 groups are referred to as the 'head' and the CH_2 groups as the 'tail'):

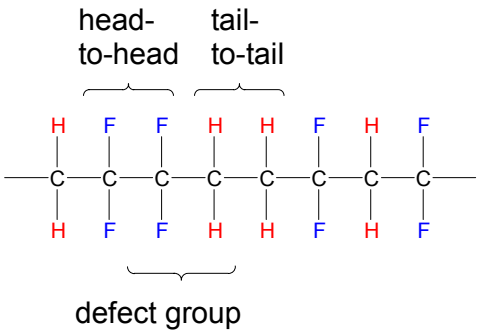

Under typical polymerization conditions the amount of defect groups is in the range 3.5 – 6%, although higher ratios of defect groups have been obtained via a special synthesis route [17]. The amount of defect groups is important as it has an influence on the crystalline structure believed to be responsible for the piezoelectric properties.

Characterization of the crystalline structure of PVDF using X-ray diffraction techniques has been well documented. Four polymorphs have been identified – these are the α, β, γ and δ phases (sometimes referred to as phases II, I, III and IV, respectively based on the order in which they were discovered). The γ and δ are not common and will not be addressed here. The α phase is the lowest energy conformation and is formed when the polymer is crystallized from the melt and is the non-polar form. The space-filling model shown in Fig. 2a is based on a distorted trans-gauche-trans-gauche' (TGTG') conformation. While there is a net dipole moment perpendicular to the chain due to the polar C-F bond, the unit cell is actually non polar.

The crystalline phase of interest for its ferroelectricity is the polar β phase. A space-filling model of the polar β phase is shown in Fig. 2b. The polymer chains are in a distorted, planar zigzag, all-trans conformation and the unit cell is polar. The energy required to form the all-trans form decreases with increasing defect groups which is why the copolymers with trifluoroethylene (TrFE) (see later section) or tetrafluoroethylene (TFE), which create artificial defects, can crystallize into the all-trans form. The point at which the all-trans form becomes more energetically favored over the TGTG' form is at approximately 10% defects [18].

Figure 2. Space-filling model of a segment of a PVDF molecule in the **(a)** α phase (trans-gauche conformation), and in the **(b)** β phase (all-trans conformation) (taken from Kepler [19])

One method of artificially introducing defects into PVDF is by use of a comonomer. A very popular comonomer is trifluoroethylene (TrFE). TrFE is like vinylidene fluoride except one of the hydrogens is replaced by an additional fluorine atom, therefore when TrFE is copolymerized with vinylidene fluoride it essentially acts as a source of defect groups so that the polymer spontaneously forms the β phase regardless of the processing method. The amount of comonomer incorporated (the composition) may be

expressed in mols or weight. A copolymer with exactly one TrFE unit for every VF_2 unit would have a molar composition of 1:1, or 50:50, whereas the weight composition would be 44:56 due to the slightly higher molecular weight of the TrFE groups. Most manufactures use weight % and not mol %, although clearly it is important to make the distinction. Throughout this report we use weight % unless specified otherwise. The Curie temperature of these TrFE copolymers varies with comonomer content. The dependence of Curie temperature and melting point on comonomer content is plotted in Fig. 3 (left). It is apparent that a linear extrapolation to 100% VF_2 content reveals that the Curie temperature of PVDF is predicted to be approximately 195 °C. A P(VDF_{63}-$TrFE_{37}$) (63:37 weight %) polymer heated through the Curie temperature experiences a reversible change from the β to α phase as indicated by the temperature dependent XRD plots in Fig. 3 (right).

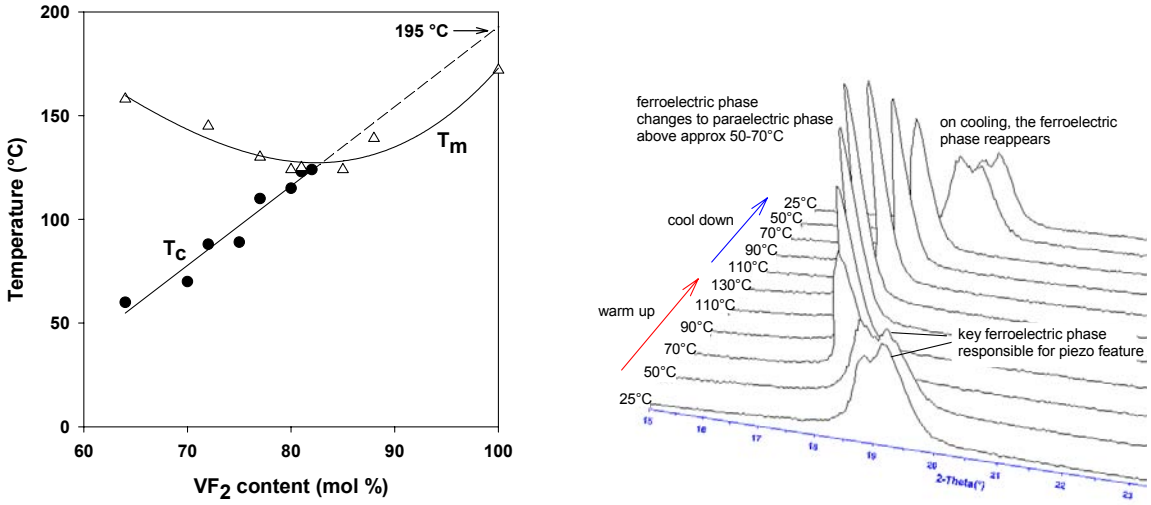

Figure 3. Melting point and Curie temperature versus molar composition of a series of TrFE copolymers [20] **(left)**; XRD plots showing phase changes with temperature for a P(VDF_{63}-$TrFE_{37}$) copolymer **(right)**

P(VDF-TrFE) has received additional attention by researchers due to unusual effects after irradiation with high doses. Zhang et al [21] extended on the work of Lovinger [20] who first observed interesting changes in the crystal structure of P(VDF-TrFE) when exposed to radiation, to report a large electrostrictive response of the irradiated polymer [21]. This discovery led Zhang and others to comprehensively investigate the effect of radiation on P(VDF-TrFE) using FTIR, X-ray, crosslinking density, DSC, DMA, mechanical measurements, solid-state NMR and various electrical techniques [22-24]. Their principle observation was that the copolymer, when subjected to electron beam radiation, is transformed from a normal ferroelectric with a large hysteresis loop to a relaxor-like ferroelectric with a slim polarization loop. The effect of the radiation is to disrupt the polar crystallites, expanding the lattice and creating nano-polar regions. This work has since been expanded with the irradiation step being replaced by either chemical crosslinking [25] or by incorporation of a third disparate monomer such as CTFE or HFP to produce nanodomains. The advantages of moving away from irradiation is that unwanted scission and other radical reactions are avoided, hence reasonable mechanical properties can be achieved. None of these electrostrictive polymers are commercially available and because they have low melting points (ca. 110 °C) and are not piezoelectric, were considered unsuitable for the proposed application. Unlike piezoelectric materials, electrostrictives have a non-linear strain response to an applied field, small operating temperature range, and do not contract when the field is reversed.

The polymer produced from polymerizing vinylidene fluoride with hexafluoropropylene (HFP) has also been examined for its piezoelectric response. Like the PVDF homopolymer, it must be stretched to obtain

the polar β-phase. Solvent-cast films of P(VDF-HFP) which were stretched and poled have been examined for pyroelectric stability [26]. It was found that samples kept at 150 °C for 5 minutes still exhibited 30-40% of their original pyroelectric effect. After the annealing step, no further decay of the pyroelectric coefficient was observed during storage at 120 °C for several hours [26]. However, no long-term aging experiments have been reported.

Of all the electroactive polymers mentioned in this section, only the PVDF homopolymer and the TrFE copolymer are commercially available as piezoelectric films. In the United States, the piezoelectric homopolymer can be obtained as film in a range of thicknesses either with or without electrodes from MSI Inc and Ktech Corp. The only source of piezoelectric TrFE copolymer film is from Ktech Corp, although MSI does sell the TrFE copolymer as powder (although it is not a standard catalogue item). Table 1 has a listing of other commercial and non-commercial sources of PVDF related polymers. The conformability, flexibility, robustness and lightness give PVDF an advantage over ceramic piezoelectrics for many applications. Some of these are listed in Table 2 [27].

Table 1. Commercial and non-commercial sources for PVDF based polymers

Polymer	Composition Available (weight %)	Supplier	Comments
PVDF	100% PVDF	Atofina	Kynar product; pellets
P(VDF-HFP)	4% and 15% HFP	Atofina	Kynar product; pellets
PVDF	100% PVDF	Solvay	pellets
P(VDF-CTFE)	19% CTFE	Solvay	pellets
P(VDF-TrFE)	37% TrFE	Solvay	Sold as 50:50; pellets
P(VDF-TrFE)	All compositions	MSI USA	many different compositions, non-standard items; powder
PVDF film	100% PVDF	Terphane	uses Solvay polymer
PVDF film	100% PVDF	Westlake	uses Kynar polymer
Custom copolymers		Prof B. Améduri at the Laboratory of Macromolecular Chemistry, Montpellier	they are able to make almost any composition of custom VF_2 polymers
Terpolymers P(VDF-TrFE-CTFE) and P(VDF-TrFE-HFP)	unknown	Francois Bauer, Institute Saint Louis, France	electrostrictive polymer
Piezoelectric PVDF film	100% PVDF	MSI USA	available in 34, 55, 110 μm films
Piezoelectric PVDF film	100% PVDF	Ktech Corp	available in 40 μm films
Piezoelectric P(VDF-TrFE)	20% and 25% TrFE	Ktech Corp	available in 25, 110 μm films

Table 2. Applications of PVDF

Application	Feature utilized
Headphone membrane/loud speakers	high frequency range (up to 10^9 Hz)
Marine fouling prevention	conformability/robustness
Strain measurements	flexibility
Contact switches	thin
Motion sensors	pyroelectricity
Active and passive vibration control/dampening	thin film/unobtrusive incorporation

3. Poling and piezoelectric property characterization

When a piezoelectric polymer is subjected to a mechanical load, positive and negative charges develop on the material surface. This ability of the material to convert mechanical energy into electrical energy is known as the direct piezoelectric effect. Conversely, a piezoelectric polymer will deform under an applied electric field. Hence, the converse piezoelectric effect is the ability of the material to convert electrical energy into mechanical energy. The direct piezoelectric effect is used in sensor applications, while the converse effect is used in actuator applications. Linear piezoelectric constitutive relations, which can be derived from thermodynamic principles, couple linear elastic relations with linear dielectric relations through the piezoelectric tensor:

$$s_{ij} = S^{E}_{ijkl}\sigma_{kl} + d_{ijn}E_n \qquad \textbf{Equation (1)}$$

$$D_n = d_{nij}\sigma_{ij} + \varepsilon^{s}_{ni}E_i \qquad \textbf{Equation (2)}$$

where s is strain, σ is stress, E is electric field, D is dielectric displacement, S is mechanical compliance tensor, ε is a permittivity tensor, and d is a piezoelectric tensor [28].

The piezoelectric effect originates from induced polarization. To induce polarization, the dipoles in a semi-crystalline polymer such as PVDF must be reoriented through the application of a strong electric field (Fig. 4) at elevated temperature. The temperature is then lowered in the presence of the electric field so that the domains are locked in the polarized state. The material's piezoelectric effect is directly related to the degree of polarization achieved. The two most common techniques to induce polarization in piezoelectric polymers are electrode and corona poling.

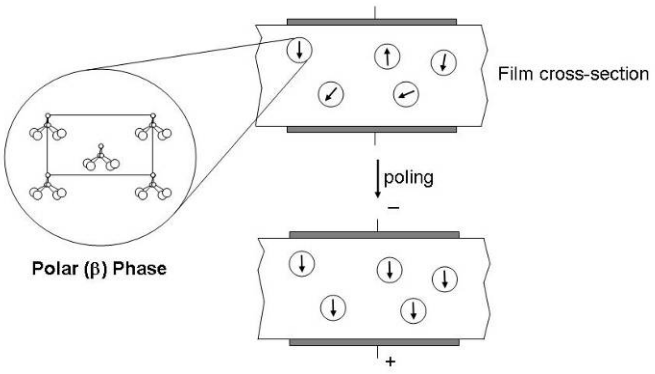

Figure 4. Reorientation of the β-phase dipoles in PVDF via poling

A schematic diagram of the electrode poling method is presented in Fig. 5. The conducting electrodes, which are either evaporated, sputtered, painted, or pressed on the polymer surfaces, are necessary for poling. For poling of PVDF films, a 600 Å layer of evaporated aluminum on each side has been found to work satisfactorily. The voltage potential applied to the electrodes produces an electric field across the sample. To prevent arcing that will permanently damage the material, the sample may be placed in a vacuum or submerged in an insulating fluid such as Fluorinert, or alternatively if the electrodes do not reach the edge of the film the poling can be done in air without arcing. Permanent (i.e. evaporated, sputtered, painted) electrodes are preferred over the pressed-on electrodes because of the superior contact between the electrodes and the sample. The poor contact in the case of pressed electrodes may lead to

local discharges, dielectric breakdown, or inhomogeneities in the poling field. The sample should be monitored for contaminants as the charges may get injected into the material at high electric and thermal fields [29].

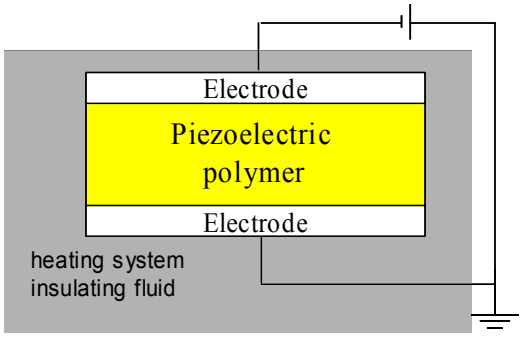

Figure 5. Schematic of the electrode poling system

Both constant and varying electric fields can be applied to the sample during electrode poling [30,31]. A constant electric field is held on the sample from 10-30 minutes up to 2 hours [32-34]. Application of high voltages for a prolonged period of time may increase the probability of dielectric breakdown, thus making a variable field procedure a more attractive alternative. The process when the material is poled through the application of a variable electric field is called "hysteretic poling" [31]. The varying electric field is usually applied at low frequency (mHz) and either sinusoidal or triangular waveforms may be used [35-38].

The schematic diagram for corona poling is presented in Fig. 6. A surface is placed on a heating plate with the bottom surface connected to the ground. A corona tip (a needle or a sharp blade) is suspended above the sample and is subjected to high (8-10 kV) voltages [39]. The dry air [40] at the tip gets ionized with the tip's polarity. When the corona discharge occurs, the ionized particles are accelerated towards the ground and are deposited on the sample's top surface. The charges remain on the surface generating a poling electric field between the top surface and the ground [29]. The magnitude of the electric field depends on the amount of charges deposited that can be controlled with a metallic grid placed between a corona source and the polymer. The grid is usually placed at the distance of 3-4 mm from the sample. The voltage on the grid may vary from 0.2 to 3 kV [41]. The advantages of the corona poling are that it is more amenable to film imperfections, electrodes are not required, and large area samples may be poled, which would be useful for the mirror application. The disadvantage is that it is considerably more difficult to setup and optimize than the direct electrode method.

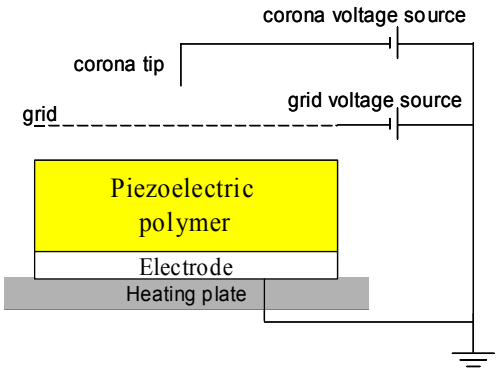

Figure 6. Schematic of the corona poling system

The magnitude of the electric field and sample temperature are important parameters in the poling process. The usual rule of thumb is the higher the applied electric field, the higher the induced polarization provided the poling field is larger than the coercive field of the material being poled. The coercive field for PVDF and its copolymers is typically between 50 and 120 MV/m (120 V/μm) [42]. Although the poling may be done at room temperature [32,36], an elevated temperature improves dipole mobility and consequently increases the material polarizability. Another issue to consider is warping of the films during the poling process due to the change in volume during orientation of the dipoles. Poling at elevated temperatures can help minimize warping due to relaxation of the polymer film and help it conform to the 'new' poled volume, especially at the boundary between the poled and non-poled areas. Unlike the poling field for which larger values will produce larger polarization, there is an optimum poling temperature that results in maximum polarization and piezoelectric properties [41,43]. Typical optimum poling temperatures are in the range 85 °C to 130 °C.

Methods for evaluation of degradation of piezoelectric properties. In evaluating piezoelectric properties of PVDF and copolymers in response to degradation effects, it is important to consider how ultimately those conditions will affect the control of the mirror. Many different methods for measuring the piezoelectric response of a material exist, some of them utilizing the direct piezoelectric response and other exploiting the converse effect. In the following section, different methods for evaluation of material properties are presented with the pros and cons of each method discussed.

Piezoelectric properties. One of the methods to measure piezoelectric constants is to apply a uniaxial stress and measure the charge generated due to the direct piezoelectric effect [28,33]. The schematic representation of the test is provided in Fig. 7. The ratio between dielectric displacement (a charge per unit area) and the stress applied allows determination of the piezoelectric constant d_{31} (or d_{32} depending on the direction of applied stress). Alternatively, if the stress is applied in the thickness direction, the d_{33} coefficient can be measured. The charge can be measured with an electrometer or a picoampmeter. Sensitivity of the electrometer requires quality electrodes attached to the sample. The electrodes are usually sputtered or evaporated thin metallic films [34,42,44]. Silver paint electrodes may also be used [35]. Thickness of the electrodes should be much smaller than the film thickness in order to avoid clamping effects. The need for deposited electrodes makes this method less attractive, however for the d_{33} measurement contact electrodes will suffice since there is no issue with clamping effects.

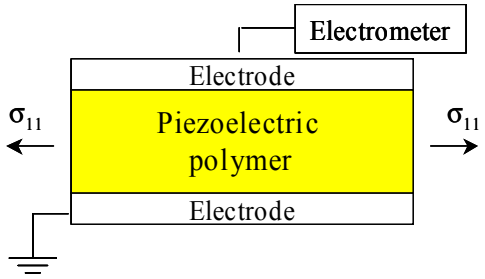

Figure 7. Schematic of a test to obtain the d_{31} piezoelectric coefficient

Another way to measure piezoelectric properties is to apply an electric field and measure the strain generated due to converse piezoelectric effects. The method is illustrated in Fig. 8. Sputtered or evaporated electrodes are required to transfer generated displacement to the strain gage. The strain gages should be used with caution since the gage thickness is of the same magnitude as the film thickness. If the sample is long enough, the changes in the overall length may be measured while avoiding the use of the strain gages [28]. If the change in thickness is to be measured a laser position sensor can be used.

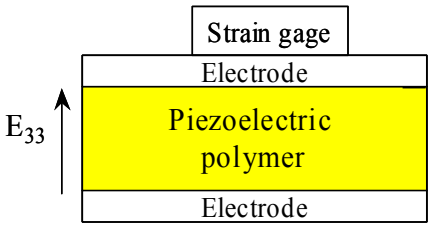

Figure 8. Schematic of a test setup for evaluation of piezoelectric constants

Possibly the most basic and the most informative test for piezoelectric performance is to measure the deformation of a bimorph. The d_{31} coefficient is related to the bimorph deformation through equation 3 where δ is the displacement of the tip, L is the length of the bimorph, t is the thickness of the bimorph and V is the applied voltage [45]. Measuring the change in δ under different conditions, for example temperature, can provide a very useful understanding of overall piezoelectric performance.

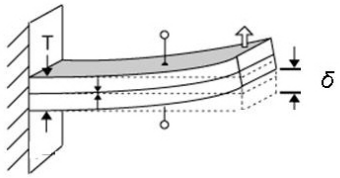

$$\delta = \frac{3}{2} d_{31} \frac{L^2}{t^2} V \qquad \textbf{Equation (3)}$$

Dielectric properties (permittivity) and ferroelectric hysteresis (D-E) are the easiest to measure for thin film samples. The schematic of the set up is represented in Fig. 9. An electric field is applied to the sample and the charge generated is measured. The charge is converted to dielectric displacement with one of the equivalent Sawyer-Tower circuits [46], a ferroelectric measurement system (Radiant Technology RT6000), or by numerical integration of the current supplied by the power supply [42]. A typical result is a square ferroelectric hysteresis loop presented in Fig. 10. Coercive field, remanent polarization, and saturation polarization are the characteristic parameters of the hysteresis loop. The parameters change upon aging, reducing the square hysteresis loop into a needle like loop. For piezoelectric ceramics, the degradation in ferroelectric hysteresis properties is analogous to degradation in piezoelectric properties. That is, percent degradation of remanent polarization is comparable to strain output degradation during ferroelectric fatigue cycling [47]. Similar correlation is expected for piezoelectric PVDF polymers. It was shown for nitrile-substituted polyimide that remanent polarization is directly proportional to the material's piezoelectric response [33]. A major benefit of this method is that simple contact electrodes such as conducting tape are sufficient.

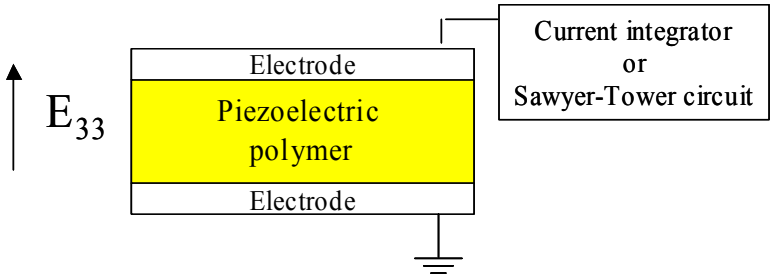

Figure 9. Schematic of experimental setup for dielectric measurements

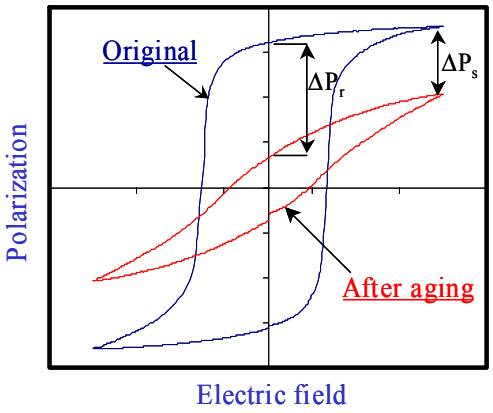

Figure 10. Typical ferroelectric hysteresis loop before and after degradation

Remanent polarization can also be measured by thermally depoling the material while measuring the released charge with an electrometer [33]. The thermal methods are advantageous to study the physics of the material but not appropriate for the evaluation of aging effects because the repeated poling needed may mask any aging effects. However, the thermal method may be attractive to investigate the degree to which polarization may be recovered after aging, or to measure the effect of radiation on ferroelectric domain structure [36].

In summary, the methods for measuring piezoelectric properties and the constants they supply are:

- direct piezoelectric effect via application of pressure (piezoelectric strain coefficients: d_{31},d_{32}, d_{33})
- bimorph deformation (d_{31}, d_{32})
- D-E hysteresis loops (remanent polarization, permittivity, coercive field)
- thermal depoling (remanent polarization)

It is obvious that many of the measurements overlap in terms of the information they provide, for example both direct and converse measurements can be used to determine the *d* strain coefficients. In choosing which measurements to use we have taken into account availability of equipment, simplicity, accuracy and reproducibility, and amount of sample required since for some of the LEO simulations only small samples could be exposed. With this in mind we have chosen the d_{33} as a very simple and rapid measure of the piezoelectric strain in the thickness direction which requires only 1 mm square samples and is non-destructive. Further, the bimorph deformation is a good visual indication of piezoelectric performance closely related to the mirror application, and D-E hysteresis loops are suitable for the wide temperature range possible and fundamental information provided.

4. Polymer characterization

In Section 3 piezoelectric characterization methods were discussed. In this section other characterization methods considered important to the performance and degradation evaluation of PVDF polymers are briefly summarized.

Traditional polymer characterization methods. Some of the simple and traditional characterization methods for evaluation of degradative changes in PVDF polymers include tensile measurements for monitoring of mechanical properties, gel analysis to measure crosslinking and scission effects due to radiation damage, film contraction measurements for stretched films to quantify residual stress in the material, and dynamic mechanical analysis (DMA) for determining the modulus over a wide temperature range. All are standard techniques commonly used in polymer degradation studies [48]. For example, tensile elongation and strength are a sensitive property that is widely used to monitor mechanical changes in polymers [48,49]. Gel content and solvent uptake analysis is based on the swelling of crosslinked polymers in the presence of organic solvents. Particularly elastomers and radiation aged materials where crosslinking is part of the degradation mechanism are amenable to this technique [50,51]. With careful experiments average molecular weights between crosslinks can be obtained [50]. Dynamic mechanical analysis can be conducted using tensile or cantilever based methods on small polymer samples. Stress is carefully applied to the sample and strain features as a function of temperature can be measured yielding moduli and phase transition data relevant to polymer chain mobility and morphology. The modulus, as will be shown in section 5.2, is an important feature to understand actuator performance and is also a critical input parameter for finite element modeling of bimorphs using these polymers. For performance predictions over a large temperature range the correlation between temperature and modulus needs to be available. Various other standard polymer characterization methods have also been employed for which the details may be found in the corresponding references at the end of this report.

Morphological analysis and crystallinity. One of the most important parameters affecting the piezoelectric properties of PVDF is the level of crystallinity. Without crystallinity or defined morphology, PVDF would not exhibit any piezoelectric properties since it could not sustain a net dipole. The level of crystallinity and associated features is also a key thermodynamic parameter affecting the mechanical, chemical and thermal properties of semi-crystalline polymers. It is therefore important to completely understand the crystallinity and morphological aspects of PVDF and copolymers. A wide range of techniques are available which have been used to determine the crystallinity of PVDF including calorimetric and spectroscopic methods. Of these techniques possibly the most widely used due to its availability in most polymer laboratories, simplicity and relative cost, is DSC (differential scanning calorimetry). By heating the polymer at a constant rate through the crystalline melting transition the heat of melting and melting points can be measured. Both parameters provide important feedback on crystalline properties. Dividing the determined heat of melting by the theoretical heat of fusion of a 100% crystalline material yields a value of the mass percent crystallinity. A potential problem arises from the fact that the theoretical heat of fusion of 100% crystalline PVDF or any of the copolymers is often not available or can only be estimated via data extrapolation. While a literature value for PVDF has been published [52], the merits of the technique and data analysis used to derive the value are somewhat questionable [53]. As for the copolymers no values have ever been reported and most researchers have used the value for the PVDF homopolymer. An alternative method for crystallinity determination, which does not require samples with known crystallinity, is X-ray diffraction analysis. The diffraction pattern created when X-rays impinge on a polymer sample can be used to determine the crystalline phases (for example, α or β) and also the level of absolute crystallinity. XRD spectra (for example, Fig. 3 (right) in section 2) contain sharp peaks due to the crystallites, while the amorphous regions give rise to a much broader background scattering. By deconvoluting the spectra into the broad and sharp components a

measure of the crystallinity can be made. One of the limitations of XRD, especially for oriented films such as the PVDF homopolymer in its piezoelectric state, is that it is difficult to distinguish between ordered structure from the crystallites and pseudo-ordered structure due to stretching. For this reason, the crystallinity determined by XRD for stretched films may be artificially high and exact quantification may be complicated.

A recently developed and superior technique for measuring the crystallinity of PVDF is by high speed solid state ^{19}F NMR spectroscopy. Because of slight chemical shift differences between the fluorine atoms present in the crystalline and amorphous regions, the spectra can be resolved into crystalline and amorphous components, which can then be used as a direct measure of the mass-percent crystallinity. Figure 11 shows two examples where spectra have been deconvoluted into crystalline and amorphous components. An important limitation of this technique is that it is dependent on separation of the peaks representing the different morphologies, and there are some issues with the definition of peak shapes to be used for mathematical peak deconvolutions.

The NMR method can also be used to gather crystallinity data at elevated temperatures. Figure 12 (left) shows the change in the spectra of P(VDF-HFP) as the temperature is increased. When superimposed with the normalized crystallinity from DSC (Figure 12 (right)) excellent agreement can be observed. It was possible to demonstrate for the first time how ^{19}F NMR can be used as a reliable method for measuring the temperature dependence of crystallinity. Ultimately this technique could lead to a much deeper understanding of important structural features in these materials and represents an intriguing opportunity for the assessments of piezoelectric responses in PVDF and copolymers and correlation with primary morphology.

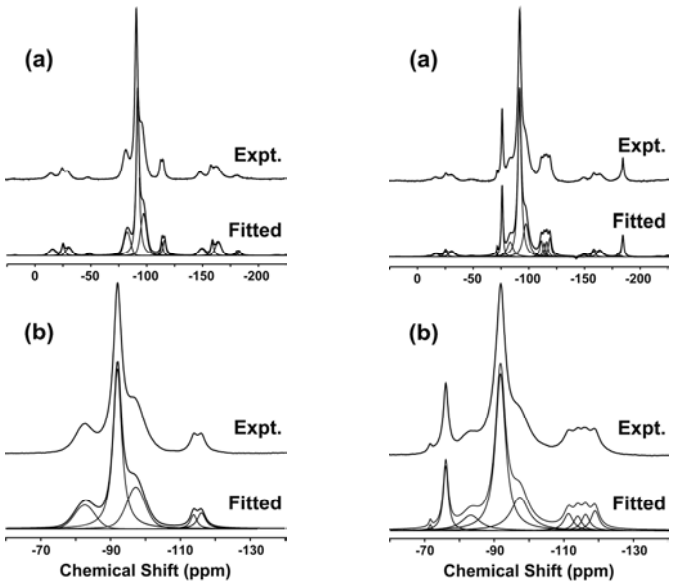

Figure 11. ^{19}F DP/MAS spectrum (v_r = 25 kHz, actual sample temperature = 53°C) of Kynar 740 PVDF film **(left)** and Kynar 2750 P(VDF_{96}-HFP_4) **(right)**. **(a)** center bands and first-order spinning sidebands, **(b)** center bands only. Both the experimental spectrum and the fitted spectrum are given. The ^{19}F resonances modeled with Lorenztian peaks which comprised the fitted spectrum are also shown.

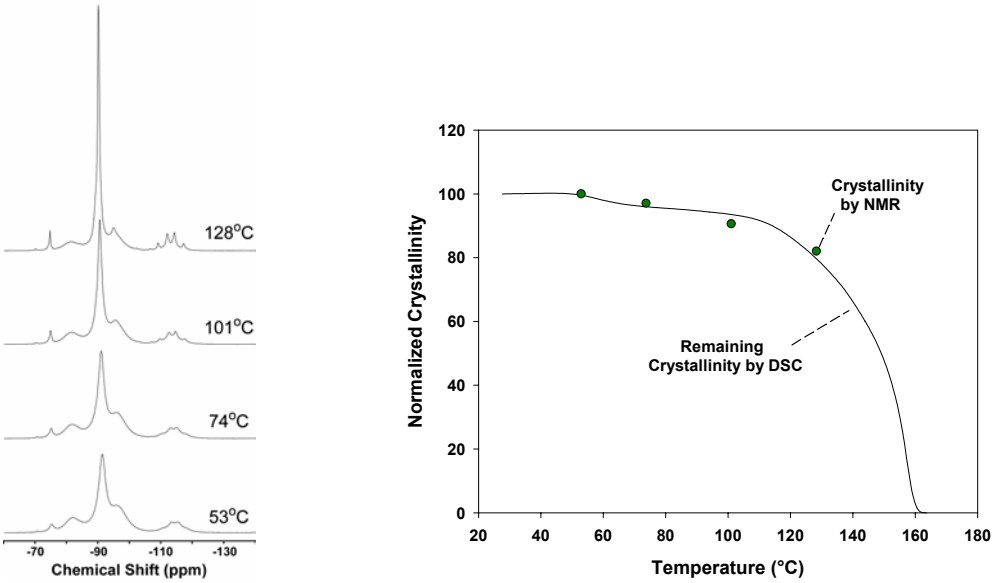

Figure 12. ^{19}F NMR spectra of P(VDF_{96}-HFP_4) acquired over a wide temperature range **(left)**; the central peak assigned to the amorphous component increases with temperature as partial melting occurs. Correlation between the crystallinity determined by NMR and the remaining crystallinity from DSC, both normalized to the initial room temperature values **(right)**

5. Performance limitations in space environments

5.1 Overview of space environmental conditions

The near-Earth space environment consists of a host of highly energetic species, which are potentially damaging to polymeric materials. Many of these species, such as photons from sunlight, particles from solar flares and galactic cosmic rays, originate from the sun and other stars. Others, such as high velocity (relative to the spacecraft) neutral gases, the Van Allen Belts, and the Ionosphere originate from the Earth or interactions between the Earth's upper atmosphere and other energetic species. The concentrations of all of these energetic species vary with altitude and are summarized in terms of importance to the success of a mission in Table 3 for the most common orbits – low Earth orbit (low and high inclination), medium Earth orbit, and geostationary Earth orbit. For the current application we are only concerned with LEO, however, if other orbits are considered in the future then obviously based on the information in Table 3, it will be important to re-evaluate the effects of other particular orbits on the materials. Of the parameters affecting spacecraft in either high or low inclination LEO orbit, the most important to consider are:

Neutral gases. The most abundant and damaging neutral gas in LEO is atomic oxygen formed by photodissociation of the small concentration of molecular oxygen in the upper atmosphere. The flux is approximately 10^{15} atoms/cm^2-s with an orbital speed of 8 km/s, which can cause surface pitting and erosion of polymers. It has repeatedly been shown that exposure of polymers to atomic oxygen causes surface erosion [5,8,11,14,54]. The mechanism, while not fully understood, is believed to be due to oxidation by the highly reactive oxygen atoms followed by volatilization of fragment molecules. When the incident AO is anisotropic (as is the case for orbiting spacecraft) this leads to a highly directional erosion process resulting in patterned surface morphology [55]. Atomic oxygen mainly affects leading edges.

Table 3. Environmental effects on spacecraft in LEO, MEO and GEO (adapted from: "Space Environmental Effects on Spacecraft: LEO Materials Selection Guide" E.M. Silverman, NASA Contractor Report 4661 [14])

Spacecraft Environment	LEO low incl.	LEO high incl. (ISS)	MEO	GEO (GPS)
Direct Sunlight	⚠⚠⚠⚠	⚠⚠⚠⚠	⚠⚠⚠⚠	⚠⚠⚠⚠
Gravity Field	⚠⚠⚠	⚠⚠⚠	⚠⚠⚠	
Magnetic Field	⚠⚠⚠	⚠⚠⚠	⚠⚠⚠	
Van Allen Belts	⚠⚠	⚠⚠⚠	⚠⚠⚠⚠⚠	⚠
Solar Flare Particles		⚠⚠⚠⚠	⚠⚠⚠	⚠⚠⚠⚠⚠
Galactic Cosmic Rays		⚠⚠⚠⚠	⚠⚠⚠	⚠⚠⚠⚠⚠
Debris Objects	⚠⚠⚠⚠⚠ ⚠⚠	⚠⚠⚠⚠⚠ ⚠⚠	⚠	⚠⚠⚠
Micrometeoroids	⚠⚠⚠	⚠⚠⚠	⚠⚠⚠	⚠⚠⚠
Ionosphere	⚠⚠⚠	⚠⚠⚠	⚠	
Hot Plasma		⚠⚠⚠		⚠⚠⚠⚠⚠
Neutral Gases	⚠⚠⚠⚠⚠ ⚠⚠	⚠⚠⚠⚠⚠ ⚠⚠	⚠	

The number ⚠ of symbols indicates the potential for damage. No ⚠ symbols means it can be ignored, 10 ⚠ symbols will negate the mission

Direct sunlight (vacuum UV). Fluorinated polymers, and particularly PVDF, are excellent materials under terrestrial outdoor exposure conditions. PVDF is in fact the base polymer for many high performance, long-lasting industrial coatings. Terrestrial UV exposure is limited to minimum wavelengths of ~ 285 nm due to protective atmospheric absorption, with the UV-B component (285-325 nm) often regarded as the most damaging for polymer performance. Many fluoropolymers do not absorb above 230-250 nm, which is the reason for their limited environmental UV degradation. Under LEO conditions, however, unprotected polymers are exposed to the full solar spectrum including the highly energetic and damaging vacuum UV components. For example, UV photon energies of 250 nm are equivalent to 478.5 kJ/mol (4.96 eV) and 200 nm to 598.2 kJ/mol (6.2 eV), respectively. Compare this with fluorine-carbon bond energies of 452 kJ/mol (265 nm) for F-CH_3, and 530 kJ/mol (226 nm) for F-C_2F_5. It is obvious that the LEO vacuum UV radiation will be extremely damaging and therefore prediction of degradation levels requires knowledge of UV irradiances. Since the early 1990s there have been two programs to measure solar UV intensities and their dependencies on solar cycles, mostly to provide data for atmospheric modeling. NASA has sponsored the two Solar Ultraviolet Spectral Irradiance Monitor (SUSIM) instruments in these SUSIM programs [56,57] providing data over more than a ten-year period. Fig. 13 shows an example of the direct (90° exposure) solar UV intensities at an average Earth to sun distance of 1.493×10^8 km. Most of the total irradiance below 150 nm is due to the Lyman-α hydrogen line at 121 nm. The integrated irradiance data have been included in Fig. 13 and provide immediate feedback on expected UV energy deposition. Starting from the lowest wavelength up to 200 nm, a total irradiance of 0.1 W/m^2 is expected, up to 227 nm a total flux of 1 W/m^2. Energy deposition in thin polymer films will depend on absorptive and reflective properties and other radiation/material interactions, i.e. energy loss and transfer processes. However, it is well established that polymer films easily absorb UV radiation (UV cut off in absorbance measurements) and that damage is

often heterogeneous, i.e. UV exposure often leads to surface cracking and embrittlement due to higher absorbance in the top layers and limited depth penetration as often reported for the weathering of films and coatings.

A simple estimation of the magnitude of UV energy deposition in LEO is accomplished by assuming the ~0.1 W/m^2 (up to 200 nm) irradiance, full energy absorption in a 100 μm thick film, and a one year exposure in a low equatorial orbit. Disregarding orbital latitude or corrections for spacecraft tilt we assume a simplistic orbit of 12 hours shadow and 12 hours of sun illumination where the 12 sun hours equate to the equivalent of ~7.65 hours of vertical sun exposure. Over a one year period the material would thus be exposed to a total of ~1 MJ/m^2 of vacuum UV photons of up to 200 nm. Assuming homogeneous energy absorption within a 1 m^2 of a 100 μm film (density is 1.7 grams/cc for fluorinated PVDF copolymers), which is equivalent to 170 grams of material, equates to 5.9 MJ/kg or 5.9 MGy per year exposure. These are significant radiation dose exposures and of course are dependent on absorption efficiencies. Not knowing real absorbances the expected radiation doses were modeled for different film thicknesses versus % absorbance (see Fig. 14) with even low %-absorbances showing significant radiation doses. These are only guidelines but clearly demonstrate the magnitude of expected radiation exposure. Considering the experimental challenges for using vacuum UV illumination for accelerated degradation experiments it would be beneficial to establish a scientific correlation between highly energetic UV irradiation and γ-irradiation. Both types of radiation are energetic enough to cause indiscriminate chain scission and are expected to display similar polymer radiation chemistry. As discussed below initial experiments to assess the radiation sensitivity of these polymers relied on γ-irradiation.

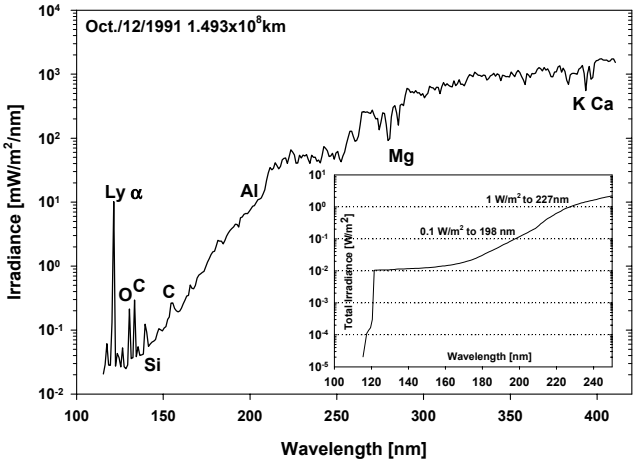

Figure 13. Low Earth orbit SUSIM based UV irradiances [56]

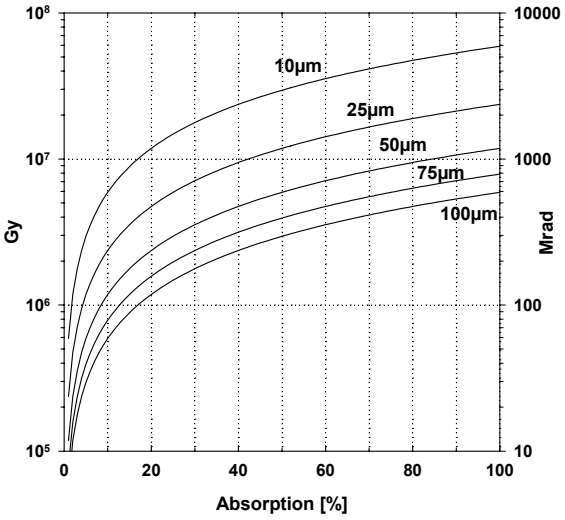

Figure 14. Predicted UV radiation doses for polymer films of different thickness over 1 year LEO exposure at (0.1 W/m^2)

While γ-photons have the potential to result in multiple radiation damage events, energy loss for the UV-photons should be limited to one or two interaction processes due to the much lower UV-photon energy. A better understanding of vacuum UV material degradation sensitivities should be a long-term goal for improved LEO exposure and performance predictions. Likewise, considering the complex LEO radiation environment with various radiation types contributing to material damage, a reasonable approach for material selection would be based on identifying the overall least radiation sensitive material. Screening studies using γ-irradiation for grading of polymer degradation are an excellent avenue for material

qualification, since a material found to withstand high doses of γ-irradiation would be expected to also perform well under strong VUV conditions.

Van Allen Belts. The Van Allen Belts consist of trapped protons and electrons of energies in the tens of keV for electrons and MeV for protons. The total doses expected are in the order of only 1 kGy per year on average based on calculations for the FEP on the HST [7]. PVDF and copolymers can easily withstand radiation doses orders of magnitude higher than this so it is not of great concern.

Solar flare particles. Protons and alpha particles from solar flares will largely be shielded by the Earth's magnetic field so that spacecraft in low inclination LEO will be unaffected to any significant degree. In high inclination LEO the dose from protons and alphas particles will be higher due to the 'open' geomagnetic field lines allowing the lower energy protons and ions to impinge on the spacecraft. It is expected that the dose will still be lower than for the protons and electrons in the Van Allen Belts, however if a high inclination mission is planned further investigation would be warranted. X-rays are also linked to solar flares but the doses are less than 1 kGy over 20 years [7].

Galactic cosmic rays (GCR). GCRs consist of alpha particles and electrons and hence have similar behavior to the solar flare particles.

Debris. This is not a materials issue and will not be covered here.

Other issues not included in Table 3, but of concern are temperature and spacecraft charging:

Temperature. The temperature of a surface directly exposed to the conditions of LEO is determined by the incident solar radiation from the sun, reflected solar radiation (albedo) from the Earth, outgoing long wavelength radiation from the Earth and the atmosphere, and a balance of these with the near-absolute zero temperature of space [14]. This balance, in turn, is a function of the ratio of solar absorbance (α_s) to thermal emittance (ε) of the material. Values of α_s and ε will vary immensely depending on the material, surface properties, and its thickness.

Spacecraft charging. Charging is not expected to cause degradation of PVDF, however it may adversely affect the control dynamics of any mirror since it may interfere with the intentional charge deposited from the electrodes. When exposed to the plasma (an electrically neutral ionized gas) present in LEO, a material will become negatively charged due to accumulated electrons stripped from the plasma. If the charge is high enough it may cause unwanted deflection of the bimorph. The extent of the charging and mitigation methods if needed should be taken into consideration during the spacecraft design.

The space environment can be extremely damaging to polymers. This is no more evident than for the Teflon-FEP used on the Hubble Space Telescope (HST) which is in LEO at an altitude of approximately 600 km. FEP is similar in structure to PVDF; it is a linear polymer containing CF_2 units, however unlike PVDF, it does not contain any hydrogen atoms which make it less radiation resistant than PVDF. FEP makes up the outer layer of the thermal insulation blankets on the HST and is therefore directly exposed to the space environment on both the sun facing and non-sun facing sides. Servicing missions after 3.6 and 6.8 years found the thermal blankets were cracked due to severe degradation as observed by the servicing astronauts and from retrieval of token samples which were evaluated in ground tests [58,59]. A taskforce was formed to investigate why FEP was degrading in LEO. The work done represents perhaps the most comprehensive body of work on effects of the LEO environment on FEP and much of what was concluded can be applied to PVDF and copolymers [6,7,10,58-61].

The main environmental factors determined to have caused the degradation of FEP were VUV, X-rays from solar flares, electron and proton radiation, and thermal cycling. The dose of X-rays, electrons and

protons was in the hundreds of Gy range, which is relatively low. The concentration of atomic oxygen at 600 km altitude is not high enough to cause erosion problems. Unfortunately, after exposing FEP to thermal cycling and synchrotron-generated X-ray and VUV radiation equivalent to the same exposure estimated for the FEP on the HST in ground tests, the amount of damage was far less than that observed in space [6]. In fact, to achieve the same amount of damage in ground tests, it took an X-ray dose equivalent to 30000 years in space. While exposures to the types of high energy radiation used in ground testing did cause damage to the FEP, clearly the effects are not well understood [6].

Part of the problem with the FEP used on the HST is that it is intrinsically a very vulnerable polymer to use in radiative space environments, in fact it is one of the more radiation sensitive polymers, even under inert conditions [62]. Fortunately PVDF is much less sensitive to radiation and it is expected that X-rays, electrons and protons in the 0.01-0.1 kGy range will have much less impact compared with what was observed for FEP. Rather than trying to account for every type of radiation present in LEO, we have used the fact that radiation damage from photons or electrons is indiscriminant of the type of radiation used, so long as the energy is sufficient enough to cause bond breakage. By exposing PVDF and other candidate materials to γ-radiation we can obtain feedback on the general *radiation resistance* in terms of how it affects mechanical and piezoelectric properties. Such an approach is far more practical than considering every type of radiation found in space individually. We believe VUV, atomic oxygen and thermal extremes will play the greatest role in the performance of piezoelectric PVDF in LEO. In the next sections the results of exposing PVDF and copolymers to these factors are presented.

5.2 Temperature effects

The surface of a satellite in LEO can experience large temperature fluctuations as a result of passing from full sun exposure to total shadow during each orbit. The actual temperatures experienced is determined by a combination of the incident solar radiation from the sun, reflected solar radiation (albedo) from the Earth, outgoing long wavelength radiation from the Earth and the atmosphere, and a balance of these with the near-absolute zero temperature of space [14]. This overall balance is a function of the ratio of the material's solar absorbance (α_s) to thermal emittance (ε). Values of α_s and ε will vary immensely depending on the material and its thickness. The multilayer insulation (MLI) blankets for the HST (made from a 127 μm thick layer of Teflon FEP with 100 nm of vapor deposited silver backing [6]) have very low α_s and high ε due to the high reflection of incident solar energy by the silver backing, and good thermal emittance of FEP [8]. With the FEP layer facing away from the Earth the polymer experiences thermal cycling from –100 to > +100 °C (estimates range from 130 °C [63] to 150 °C [8]) every 96 minutes as the satellite passes in and out of the Earth's shadow. If the aluminum side of the MLI blanket, however, is facing the sun then the temperature can reach 200 °C due to the lower emittance from the aluminum surface, as happened when a part of the blanket peeled off and curled over. Such a dramatic change illustrates how important the sun-facing layer can be in determining the temperatures experienced in an environment without convective cooling.

A remote-controlled deformable mirror made from a PVDF-based bimorph will invariably be multi-layer in nature made up of piezoelectric films, adhesive layers, and metallized layers for electrodes and reflective surfaces. The values of α_s to ε, and thus the actual temperatures experienced, will depend on the film thickness, materials used and the order in which they are layered, the thermal mass and the orbit. For this study we have assumed that the piezoelectric polymer film in LEO could experience temperatures between -100 and +130 °C in a worst-case scenario. It is recommended that a full thermal model analysis be conduced on the final mirror design as temperature will govern the performance of piezoelectric PVDF.

We were able to immediately eliminate many of the piezoelectric polymers from the materials available based on their thermal properties (melting point, Curie temperature). From the DSC traces in Fig. 15 is it clear that the HFP copolymer with 15 weight % HFP can be eliminated due to its relatively low melting point (onset ca. 110 °C), while the 4 weight % HFP copolymer should be considered as it does not begin to melt until 140 °C. Likewise the homopolymer has a very high melting point and should also be considered. For the TrFE copolymers, in addition to the melting points, the Curie transitions are also observable in the DSC traces. Obviously, the copolymers with Curie transitions below 100 °C will not perform in a space environment where the temperature approaches this value. Preferably the Curie transition should be as high as possible – of the TrFE copolymers studied the 80:20 (weight %) copolymer should have the best high temperature performance of the TrFE copolymers based on the Curie transition. The electrostrictive irradiated copolymers, mentioned briefly in section 2, can also be eliminated as they have low melting points around 110 °C, and additionally the control of electrostrictives is not as good as for piezoelectrics. This, however, has not prevented other researchers from considering these polymers for low temperature infrared telescope mirrors [64].

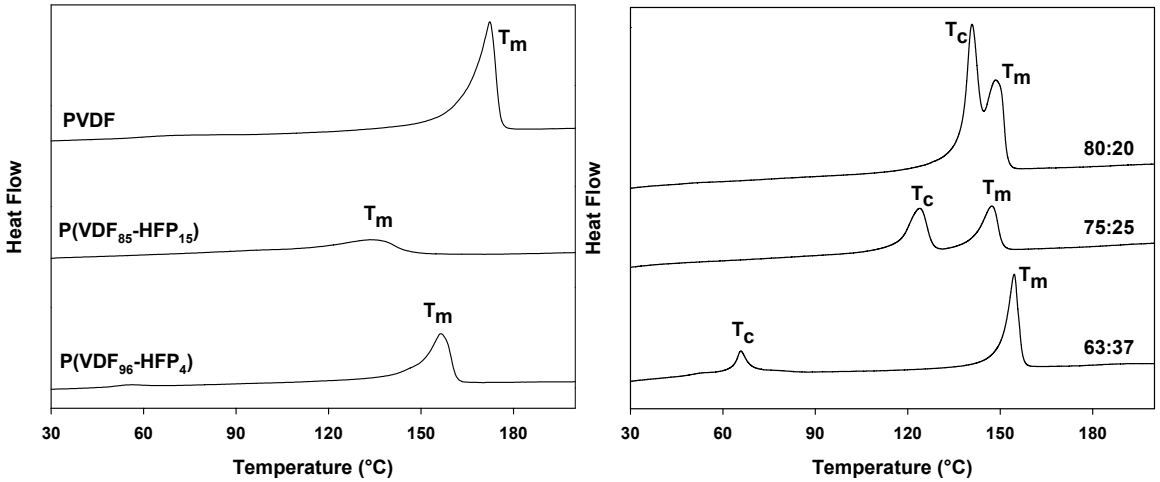

Figure 15. DSC traces of PVDF, two HFP copolymers **(left)**, and three TrFE copolymers with different weight % comonomer composition **(right)**

We began the temperature study examining three vinylidene fluoride based polymers – the PVDF homopolymer, a high melting point/high Curie temperature TrFE copolymer, and a HFP copolymer with a small percentage comonomer. The homopolymer and the TrFE copolymer were available as commercial piezoelectric films, the HFP copolymer, however, was only available in pellet form and was processed into a piezoelectric film by melt pressing, stretching and poling. After poling the d_{33} coefficient (the piezoelectric strain coefficient in the thickness direction) was measured (Fig. 16). Below a poling field of 75 MV/m there is negligible orientation of the dipoles, while between 100 and 200 MV/m there is a rapid increase in the orientation as indicated by the increase in the d_{33} coefficient which reaches a plateau above 200 MV/m. Fields above 310 MV/m could not be used due to break-down of the samples. All further experiments used HFP films that were poled using a field of 250 MV/m (250 V/μm).

To investigate the effects of thermal annealing on the piezoelectric properties of the three polymers, films were annealed at a range of temperatures below the crystalline melting point for 24 hours, cooled in air to room temperature and the d_{33} coefficient measured. Annealing is expected to cause relaxation and reorientation of the polymer chains which is anticipated to affect the piezoelectric properties. Annealing also typically results in an increase in the crystallinity of the polymer. Figure 17 shows that annealing at elevated temperatures causes thermal depoling as indicated by the loss in the d_{33} coefficient of all three

polymers. The homopolymer, while having the highest initial d_{33}, has poor d_{33} retention above 80 °C as expected based on the manufacturer's specifications and other literature reports [65]. After annealing at 140 °C the polymer retains only 32% of its original d_{33} value. The HFP copolymer has the lowest initial d_{33} and the poorest stability at elevated temperature – after annealing at 140 °C, only 15% of the original level remains, while the TrFE copolymer retains 63% of the original value after annealing at 140 °C. After annealing between 140 °C and 150 °C, the d_{33} rapidly drops to almost zero.

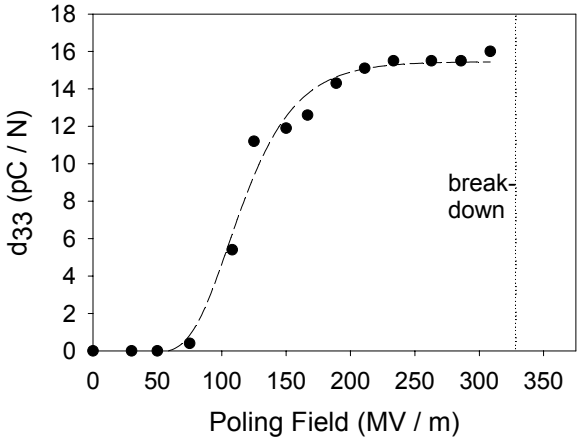

Figure 16. Change in the d_{33} coefficient of P(VDF_{96}-HFP_4) with poling field

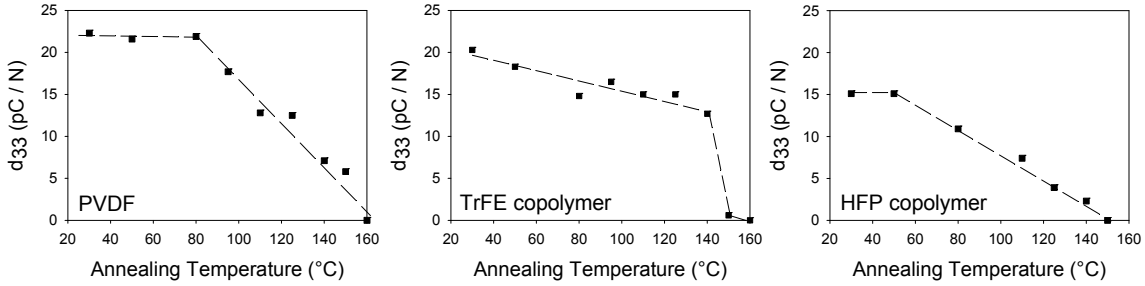

Figure 17. Change in the d_{33} coefficient with annealing temperature for PVDF, P(VDF_{80}-$TrFE_{20}$) and P(VDF_{96}-HFP_4)

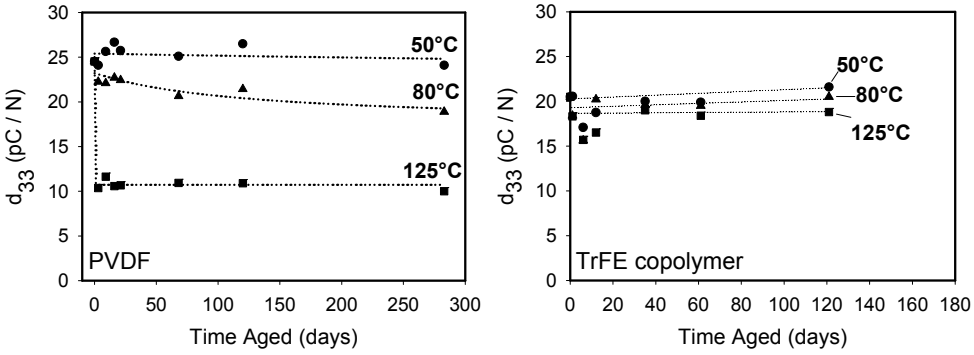

Figure 18. Long term aging experiment of the PVDF homopolymer and the P(VDF_{80}-$TrFE_{20}$) copolymer

The lower initial d_{33} of the HFP copolymer is most likely related to issues of film preparation. Previous work has shown that the conditions used when solvent casting or melt pressing, and hence morphology, can have a large influence on the piezoelectric properties of the HFP copolymer films [66].

Long-term annealing experiments were also performed on the PVDF homopolymer and the TrFE copolymer (Fig. 18). It should be noted that the PVDF reported in Fig. 18 is from a different batch than the homopolymer used in the rest of this study, hence the initial d_{33} is slightly different. It is evident that a short period at elevated temperature causes a rapid drop in d_{33} of the homopolymer, after which an equilibrium is reached and it remains unchanged. The long-term annealing experiment for the TrFE copolymer shows that the d_{33} changes very little within the error of the measurement at the temperatures studied. The ranking of the d_{33} stability of the annealed samples (that is, TrFE copolymer > PVDF > HFP copolymer) is contradictory to the respective Curie temperatures of the polymers. PVDF has the highest Curie temperature, estimated to be above the melting point at 195-197 °C [18], while the TrFE copolymer has a much lower Curie temperature of 141 °C based on DSC analysis. The Curie transition of the HFP copolymer has to be estimated since it is not observable by DSC. Preliminary results from solid-state NMR analysis suggest that the bulky HFP units are excluded from the crystallites, forming a crystal structure similar to PVDF, hence it is reasonable to assume that the Curie temperature is also above the melting point, analogous to the PVDF homopolymer.

Using a dipole model to explain the piezoelectric effect in these polymers, two requirements must be satisfied for a piezoelectric response, namely, there must be a polar phase present (in this case the all-trans conformation), and there must be co-operative orientation of these polar phases to generate a net dipole moment (this orientation takes place during the poling process). FTIR results show that below the Curie transition there is insignificant change in the trans and gauche bands [67], therefore the loss in d_{33} at temperatures below Curie transition must be due to randomization of the dipoles rather than a change from the β-phase to the α-phase.

All three films used were oriented to various degrees. The two commercial films were biaxially stretched, while the HFP copolymer was uniaxially stretched. The physical reorientation of the crystallites which must occur when the films contract will directly contribute to, and control, the depoling. A measure of the residual internal stresses within the films was obtained from the change in film area due to contraction at elevated temperatures. It was found that the stresses in the HFP film were far greater than in the PVDF film. The stresses in the PVDF film, in turn, were greater than in the TrFE copolymer film which exhibited negligible contraction at elevated temperatures. This result suggests that the TrFE copolymer film retains very little of the manufacturing stresses. It is for this reason that the less stressed TrFE copolymer film has greater thermal stability of the piezoelectric effect below the Curie transition compared with the highly stressed PVDF homopolymer and HFP copolymer. This result is supported by Wang's findings that PVDF films held in tension have slower piezoelectric decay at elevated temperatures compared with stress-free films due to the retardation of molecular relaxation [68]. In the case of the TrFE copolymer, the eventual sudden drop in d_{33} between 140 and 150 °C can be attributed to the sample reaching the Curie temperature, and certainly represents an upper use temperature.

D-E hysteresis loops were measured for the films before and after annealing and found to agree well with the d_{33} measurements. The D-E loops have the advantage that it is relatively straight-forward to perform them at elevated or sub-ambient temperatures by heating or cooling the non-conductive electronic liquid around the sample. By doing so we determined that at high temperatures the TrFE copolymer retained higher remanent polarization compared with the homopolymer, while at low temperatures the remanent polarization approached zero below the T_gs at approximately -40 °C for both polymers.

A practical device for space applications made from piezoelectric PVDF materials will invariably be in the form of a bimorph, so it is of interest to examine the thermal performance of bimorphs made from

PVDF polymers over a wide temperature range and correlate the results with the d_{33} and D-E loop annealing studies. The d_{31} coefficient can be calculated from equation 4 where δ is the displacement of the tip, L is the length of the bimorph (i.e. 31.5 mm), t is the thickness of the bimorph and V is the applied voltage [45]. Given that the applied voltage can be substituted with the driving field (E_d) multiplied by t (i.e. 60 µm for PVDF bimorph and 59 µm for the TrFE bimorph) then equation 4 can be rearranged to result in equation 5. Using equation 5, the $d_{31(PVDF)} = 28 \pm 3$ pC/N and the $d_{31(P(VDF\text{-}TrFE))} = 18 \pm 2$ pC/N.

$$\delta = \frac{3}{2} d_{31} \frac{L^2}{t^2} V \qquad \textbf{Equation (4)}$$

$$d_{31} = \frac{\delta}{E_d} \Big/ \frac{3}{2}\left(\frac{L^2}{t}\right) \qquad \textbf{Equation (5)}$$

The effects of temperature on the d_{31} coefficient for non-annealed and annealed bimorphs made from the homopolymer and from the TrFE copolymer, respectively at a driving field of 5.8 MV/m over the temperature range -95 °C to +80 °C are presented in Fig. 19. Included in the figure are superimposed moduli of the two non-annealed materials measured using differential mechanical analysis (DMA). The magnitude of the homopolymer bimorph deflection over the temperature range studied clearly depends on the modulus of the material. For larger bimorphs it is also likely that thermal expansion will have an influence on the deformation behavior (see section 6). Below the glass transition temperature the bimorph stiffens and the deflection decreases, while at high temperature any thermal depoling is compensated by the softening of the materials and results in greater deflection. A similar correlation between the d_{31} coefficient (determined from the polarization when a stress was applied) and the modulus for PVDF was reported by Wang [65]. The TrFE copolymer has a much less pronounced glass transition at approximately -30 °C and as a result, has improved low temperature deflection compared with the homopolymer.

Above 80 °C the bimorphs have a tendency for considerable warping, making tip deflection difficult to measure. Hence, for this study, bimorphs were annealed for 24 hours at 110 °C and 140 °C between thick sheets of Teflon to prevent warping and enable further measurements. The influence of annealing on the bimorphs is also included in Fig. 19. As seen in the d_{33} annealing studies, the TrFE copolymer bimorph exhibits better thermal stability of the piezoelectric properties compared with the homopolymer.

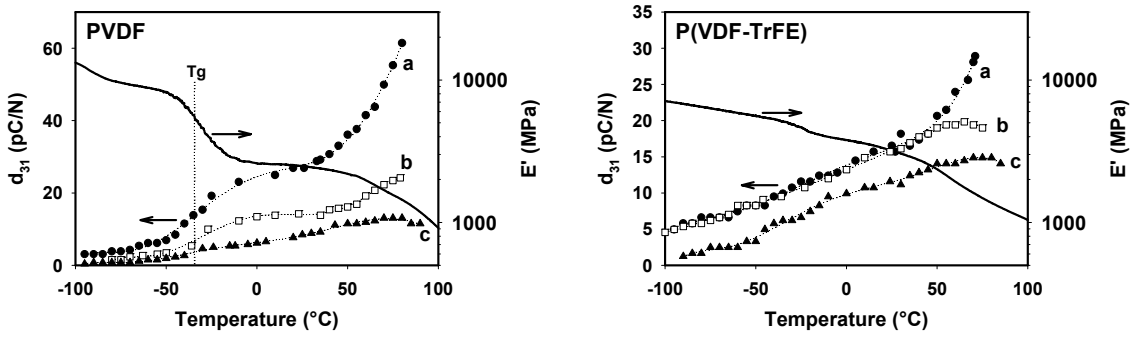

Figure 19. Effect of temperature on d_{31} coefficients and storage moduli (E') of PVDF homopolymer bimorph and TrFE copolymer bimorph **a)** unannealed, **b)** annealed 24 hrs at 110 °C, **c)** annealed 24 hrs at 140 °C

In conclusion, three PVDF-based polymers have been used to examine the influence of temperature on the piezoelectric properties via d_{33} measurements and D-E hysteresis loops. Loss in d_{33} coefficients due to thermal annealing was attributed to randomization of the dipoles and consequentially loss of polarization. The stability of the polarization in decreasing order was: TrFE copolymer>PVDF>HFP copolymer, although the processing history of the HFP copolymer was not optimized to favor high temperature piezoelectric stability. The P_r of the TrFE copolymer was more stable than the PVDF homopolymer over the range –80 °C to 110 °C which correlated with the deformation of bimorphs over a similar temperature range. Besides other LEO environmental limitations these materials have the potential to operate at the temperatures anticipated in LEO. The reported upper use temperature of PVDF of 80 °C is overly conservative and the material retains residual but still useful piezoelectric properties at higher temperatures for extended periods of time.

Unlike radiation damage due to vacuum UV and atomic oxygen exposure in LEO, the depoling of the polymers on exposure to elevated temperatures is attributed to a physical randomization of the poled domains, rather than a chemical degradation process.

5.3 Atomic oxygen and vacuum UV radiation effects

In LEO the high flux of atomic oxygen (AO), (approximately 10^{15} atoms/cm^2-s with an orbital speed of 8 km/s) formed by photo-dissociation of the small concentration of molecular oxygen in the upper atmosphere, causes surface pitting and erosion, with rates of 0.35×10^{-24} cm^3/atom for FEP and 3.0×10^{-24} for Kapton, having been reported [8]. The two commonly used techniques for simulating the atomic oxygen found in LEO are: a) hyperthermal or fast atomic oxygen [69-71], and b) oxygen plasma [11,55]. In this study the oxygen plasma method, provided by the facility at NASA Glenn, was utilized using an electron cyclotron resonance (ECR) plasma source to produce neutral atomic oxygen.

The two most promising vinylidene fluoride polymers, PVDF homopolymer and TrFE copolymer were exposed to AO exposures representing the equivalent leading edge, or ram direction AO fluence of approximately 1, 2 and 3 years at an arbitrary circular orbit of 470 km altitude [7]. In addition to the AO exposure, the samples were subjected to VUV radiation over the range 115-200 nm with an intensity equivalent to between 2.5 and 2.8 suns. The total number of equivalent vertical sun hours for the three AO exposures was on average 43, 82 and 123 hrs, respectively. The ratio of the AO fluence to VUV exposure mimics that of a surface receiving a large AO exposure (for example, in the ram direction) and little solar exposure (for example, mostly in the shade). Other than the heating effects of the VUV lamps there was no temperature control to simulate the extreme temperatures a satellite surface would experience passing in and out of the Earth's shadow.

After exposure to AO/VUV in the simulation facility, both the PVDF and P(VDF_{80}-$TrFE_{20}$) films (the only TrFE material used in these experiments) experienced significant weight loss and a decrease in thickness. In Fig. 20 the remaining percentage weight is plotted against the atomic oxygen fluence and the time in years this represents. A linear extrapolation of the points in Fig. 20 shows that for these approximately 30 μm films, complete consumption of the films will occur within approximately 5 years if they receive 100% of the ram exposure at 470 km altitude. Obviously the samples will last longer if they are thicker, if they are not on the leading edge, or if a higher altitude (where the AO concentration is lower) is used.

The erosion yield, E (cm^3/atom), defined as the amount of material lost per incident atomic oxygen atom, was calculated using equation 6, where Δm (g) is the change in the mass caused by exposure, ρ (g/cm^3) is the density, F (atoms/cm^2) is the Kapton effective atomic oxygen fluence, and A (cm^2) is the exposed surface area. The average erosion yield of all three PVDF samples was 2.8×10^{-24} cm^3/atom, while for the P(VDF-TrFE) samples the average was 2.5×10^{-24} cm^3/atom. While there are no data available for PVDF

in actual LEO, Tedlar (polyvinyl fluoride, $(CH_2\text{-}CHF)_n$), has been flown on the Space Shuttle and erosion yields between 1.3 and 3.2×10^{-24} cm^3/atom were reported [14]. Given the similarities in structure between PVDF, P(VDF-TrFE) and Tedlar, the values determined here appear reasonable. As a further comparison, the erosion yield of PVDF (which has the same overall chemical composition as an alternating copolymer of tetrafluoroethylene and ethylene) lies between that reported for poly(tetrafluoroethylene) (0.20×10^{-24} cm^3/atom) and poly(ethylene) ($3.97 \pm 0.23 \times 10^{-24}$ cm^3/atom) [8]. The values reported here for PVDF and P(VDF-TrFE) place them at the more sensitive end of the scale of erosion yields for polymers.

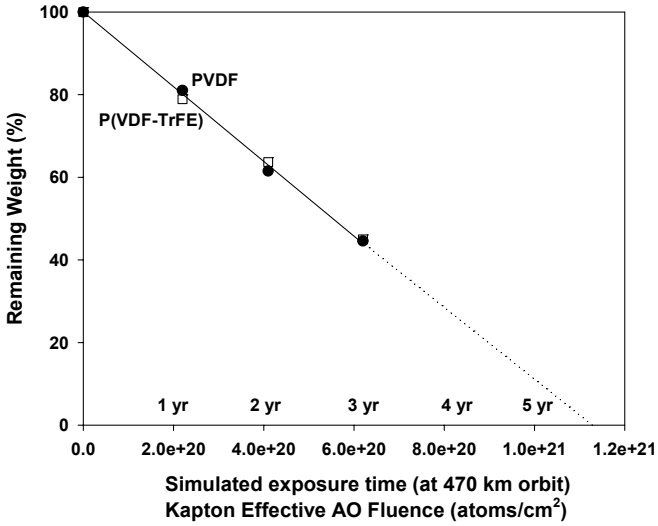

Figure 20. Change in weight of PVDF and P(VDF_{80}-$TrFE_{20}$) films after exposure to AO/VUV; extrapolation to zero weight intercepts the time axis at approximately 5 years.

$$E = \frac{volume\ of\ material\ lost}{total\ number\ of\ incident\ O\ atoms} = \frac{\Delta m / \rho}{F \cdot A} \qquad \textbf{Equation (6)}$$

Scanning electron microscopy (SEM) was used to examine the changes in the surface texture before and after exposure to AO/VUV (Fig. 21). The homopolymer exhibits a pattern slightly different to the usual 'pitting' or 'cone' formation observed for other AO-treated hydrocarbons [55]. Because of the isotropic arrival of the AO to the samples in the simulation facility used here, the formation of vertical 'pillars' observed in LEO-exposed Kapton [55] or poly(chlorotrifluoroethylene) [8], for example, are not observed. Instead, it appears that the AO preferentially erodes the less dense amorphous polymer material, emphasizing the highly oriented crystalline domains. The orientation in the PVDF films is a result of the processing required to render them piezoelectric. Stretching the films must be employed during manufacture to convert the non-polar crystalline phase to a polar crystalline phase where the protons and fluorine atoms reside on opposing sides of the carbon backbone. Poling of the stretched film by application of a large electric field results in a piezoelectric film by macroscopic orientation of the polar domains [67].

In comparison, the micrographs of the P(VDF-TrFE) films (Fig. 21), which experienced similar mass loss to the PVDF films, show surface roughening, but less pronounced patterning and no evidence of film orientation. Unlike the homopolymer, P(VDF-TrFE) does not require stretching to generate a polar crystalline phase.

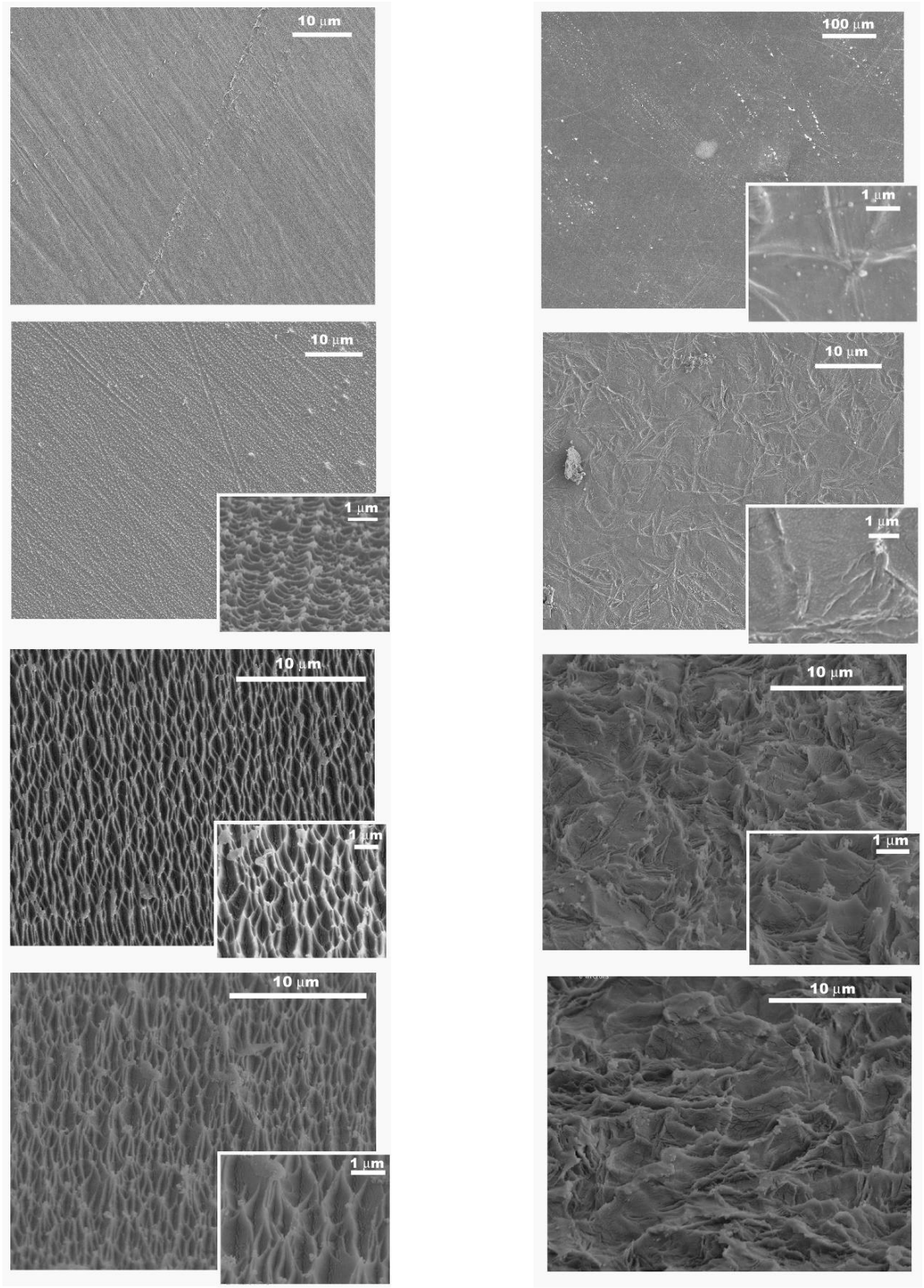

Figure 21. SEM micrographs of PVDF **(left)** and of P(VDF_{80}-$TrFE_{20}$) **(right)**. From top to bottom: unexposed, 1, 2 and 3 years simulated exposure

The surface erosion and roughening effects caused by AO exposure can be tolerated to a certain extent so long as the piezoelectric responsiveness of the films remains. Using the piezoelectric strain coefficient in the thickness direction (the d_{33} coefficient) as an indicator, the piezoelectric response of the films was measured. After AO/VUV exposure and before any thermal annealing the d_{33} coefficients of the PVDF and P(VDF-TrFE) decreased only slightly (as indicated by the data measured at 30 ºC in Figs. 22a and 22b).

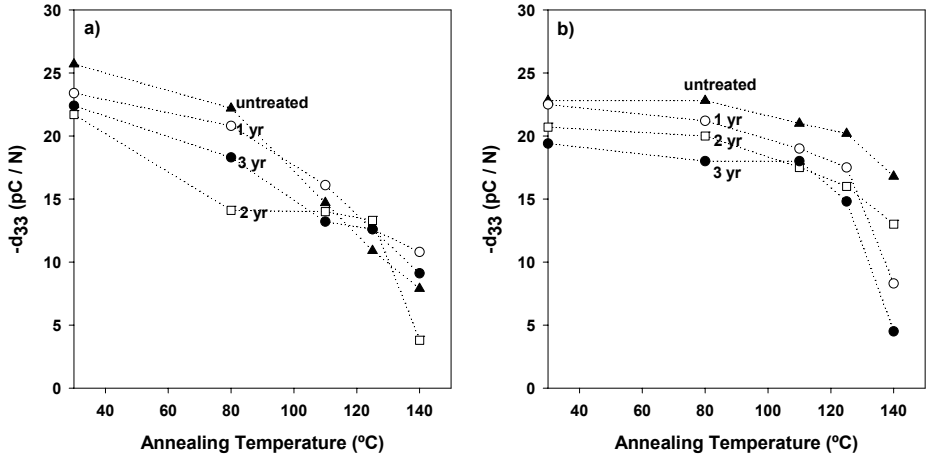

Figure 22. Change in the piezoelectric strain coefficient d_{33} with annealing before and after AO/VUV exposure **(a)** PVDF, **(b)** P(VDF_{80}-$TrFE_{20}$)

Additional thermal annealing of the AO/VUV treated samples was performed to simulate the high temperatures expected in LEO [72]. As reported earlier, PVDF, when exposed to elevated temperatures suffers an almost linear decrease in the d_{33} coefficient with increasing annealing temperature [73]. This has been attributed to contraction of the films and randomization of the piezoelectric domains resulting in loss of the macroscopic polarization. The AO/VUV exposed and annealed samples here have significant scatter in the d_{33} values, however, while not commenting on individual points, the trend is similar to the untreated film when annealed – namely, progressive depoling with increasing temperature (Fig. 22). Importantly, the AO/VUV exposure does not appear to have significantly changed the remaining bulk material of the piezoelectric properties of the films.

Thermal annealing of the P(VDF-TrFE) films also results in a decrease of the d_{33} coefficient, however, rather than a consistent decrease with increasing annealing temperature, as for the PVDF films, the d_{33} decreases slightly up to 125 ºC annealing, and then drops rapidly between 125 and 140 ºC (Fig. 22). It was shown that the films contract very little during annealing, so that the depoling is minimized below 140 ºC [73]. At 140 ºC, however, there is a sudden drop in the d_{33} as the onset of the Curie temperature (the temperature above which the polymer changes from ferroelectric to paraelectric as a result of thermal agitation) is reached (T_c = 141 ºC). AO/VUV exposure has the effect of lowering the d_{33} coefficient before and after annealing. This decrease in piezoelectric properties is especially pronounced after annealing at 140 ºC as illustrated by the 3 year sample annealed at 140 ºC which has a d_{33} of only 5 pC/N (compared with 16 pC/N for the 140 ºC annealed sample with no AO/VUV exposure) (see Fig. 22). The unexposed material was also annealed previously with the absolute properties (Fig. 17) showing some scatter due to variability in the d_{33} determinations.

To understand the greater loss in d_{33} at 140 ºC of the treated P(VDF-TrFE) material we examined the change in T_c using DSC. It was found that the onset of T_c shifts from 137 ºC for untreated P(VDF-TrFE)

to progressively lower temperatures for the 1, 2 and 3 year samples of 134, 130 and 125 ºC, respectively. The shift in T_c may be attributed to structural changes in the polar domains via some penetrating VUV radiation and chemical damage to the polymer. While no measurements were done testing the tensile strength, it was noted that the very thin 2 and 3 year samples appeared fragile and tore easily, suggesting that significant degradation had indeed occurred.

The VUV radiation component from the deuterium lamps of the AO/VUV treatment covered the range 115 – 200 nm (1040 kJ/mol (10.8 eV) to 598 kJ/mol (6.2 eV)) with an intense peak at 160 nm. Both PVDF and P(VDF-TrFE) absorb strongly below 200 nm, therefore there is a high probability of photo-chemistry during VUV exposure. Irradiation of PVDF under inert atmosphere is known to cause predominantly crosslinking and little chain scission due to hydrogen activity of the CH_2 group [62]. This is in contrast to fully fluorinated polymers such as PTFE, FEP and PFA, which undergo mainly chain scission due to the absence of abstractable protons [9,62,74]. The VUV radiation used here is more than sufficient to cleave C-F, C-C and C-H bonds present in PVDF and P(VDF-TrFE). It is therefore reasonable to assume that the VUV radiation, if significant in dose and sufficiently penetrating, will cause crosslinking of both polymers, although it is unclear what effect the simultaneous surface recession would have. None of the exposed samples exhibited the usual discoloration typically seen in polymers exposed to high energy radiation (such as γ-radiation) due to color centers [75] suggesting the absence of complex excited species or conjugated unsaturation.

To test for crosslinking after exposure, sol-gel experiments were performed. Interestingly, the copolymer had gel present after all exposures, whereas the homopolymer contained only very small gel content after 3 years of simulated exposure. Undoubtedly the mechanism is complex due to the simultaneous erosion and crosslinking. Experiments exposing the two polymers to *only* VUV radiation have also been performed and it was observed that the amount of crosslinking in the homopolymer was approximately 5 to 30 times lower than the copolymer suggesting much greater energy absorption and radiation chemistry in the latter. PVDF, with its highly alternating backbone which minimizes electronic delocalization [76], is commonly used in terrestrial applications due to its high transparency to UV-vis radiation [77]. P(VDF-TrFE), conversely, has shorter run lengths of alternating CH_2-CF_2 due to the randomly distributed CHF groups which may lower the transparency. French et al have documented the importance of alternation on transparency of fluoropolymers to VUV radiation [76]. The assumption that P(VDF-TrFE) absorbs more strongly in the VUV range than PVDF has yet to be validated experimentally due to the instrumental difficulties in measuring the VUV spectra in the range 115 – 200 nm of semi-crystalline materials. Already, it can be concluded that the results from the DSC and sol-gel measurements point to the P(VDF-TrFE) copolymer being more susceptible to radiation-induced crosslinking than the PVDF homopolymer, perhaps an indication of the increased activity of the C**H**F hydrogen in the copolymer.

In conclusion, the effects of AO/VUV exposure of two vinylidene fluoride based polymers have been examined. In both cases significant weight loss and surface erosion resulted from AO attack. Erosion yields were 2.8×10^{-24} cm^3/atom for PVDF and 2.5×10^{-24} cm^3/atom for P(VDF-TrFE), consistent with previous literature data for similar materials. The film orientation of PVDF samples was reflected in the surface topology features after exposure, while the less orientated P(VDF-TrFE) samples had less regular surface patterning after exposure. The copolymer P(VDF-TrFE) showed a greater affinity for crosslinking due to the VUV radiation when compared with the PVDF homopolymer. Most importantly, the mechanical (tensile modulus) and piezoelectric properties in the remaining bulk material of both polymers were not significantly altered, while a decrease in the Curie transition of the copolymer resulted in poorer high temperature orientation of polar domains and hence material performance after exposure to AO/VUV.

Another issue worthy of comment is a potential problem with operation of a bimorph in LEO, with a continuous electrode on one side and electrode patches on the other side for more individual position

addressing. This design may be particularly susceptible to AO erosion due to undercutting effects. Banks et al. found that a double aluminized (1000 Å thick on either side) Kapton (25 μm) blanket used on the ISS photovoltaic array box suffered complete AO erosion of the Kapton after only one year leaving only the aluminum layers (Fig. 23) [78]. The reason is thought to be due to defects in the space exposed aluminized surface allowing AO to erode undercut cavities. If the undercut cavity extends downward to the bottom aluminized surface, then the AO becomes somewhat trapped and has multiple opportunities for reaction until it either recombines, reacts, or escapes through defects in the aluminum. This is illustrated in Fig. 23. PVDF and the TrFE copolymer have similar AO erosion rates to Kapton (2.5-2.8 x 10^{-24} cm^3/atom AO for PVDF and 3.0 x 10^{-24} cm^3/atom AO for Kapton) suggesting it is likely that similar damage profiles will be observed for double metallized PVDF. PVDF with aluminum or gold on both sides will be flown on the MISSE-6 experiment (section 7.1) which will confirm if undercutting will be a problem and if AO resistance strategies (POSS, SiO_2/polymer coatings; covered in section 7.2) need to be utilized.

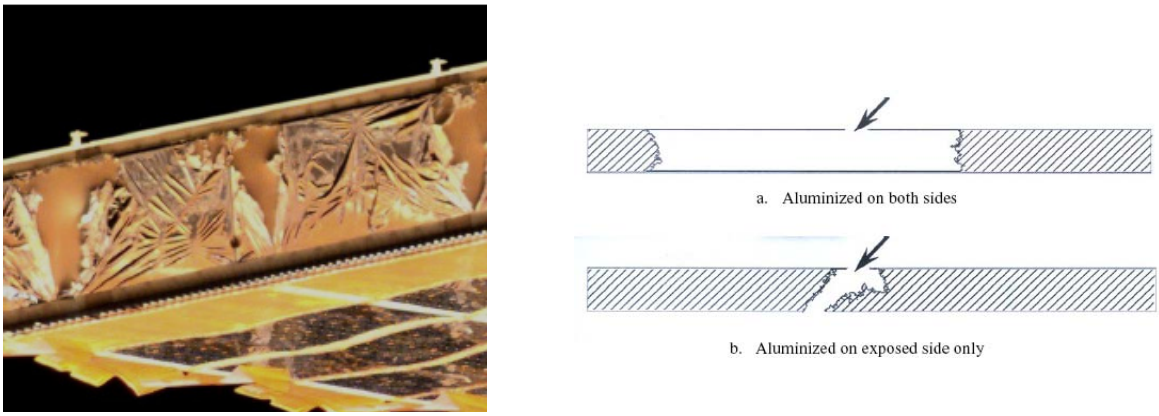

Figure 23. Under cutting effects of double aluminized Kapton on the ISS photovoltaic array box show complete erosion of the Kapton layer **(left)**; Monte Carlo simulation comparing double aluminized with single aluminized Kapton during AO attack, from Banks et al.[78] **(right)**

5.4 High energy radiation effects

In section 5.1 we mentioned that rather than trying to expose every candidate material to the many types of radiation found in LEO, it would be better to apply a general approach of determining the overall radiation sensitivities of the candidate materials using an accessible form of radiation, such as γ-radiation.

The radiation chemistry of the homopolymer, PVDF, is well established and is covered in two excellent reviews [62,79]. Fully fluorinated (perfluorinated) polymers, such as poly(tetrafluoroethylene) (PTFE) [80], experience dramatic degradation and loss in tensile properties even after relatively low (<20 kGy) radiation doses in vacuum due to almost exclusive chain scission reactions. The mechanism is believed to involve scission of C–F bonds, generating highly reactive $F^{\bullet}$ radicals which then cleave C–C bonds producing saturated end groups and terminal double bonds [62]. In comparison, PVDF retains reasonable tensile properties after irradiation at ambient temperature over a large dose range due to the presence of abstractable hydrogen atoms allowing for net crosslinking [65,81]. The crosslinks are typically H-type with *G*(*crosslinking*)- and *G*(*scission*)-values in the range of 0.95 – 1.05 and 0.2 – 0.4, respectively. (The *G*-value is defined as the number of events per $16x10^{-18}$ J (100 eV) of absorbed energy). In addition to crosslink formation, unsaturation and HF evolution have been observed. Changes in the crystallinity have also been studied and found to increase after low dose irradiation and then decrease slightly when exposed to higher doses [82,83]. Formation of small crystallites in the amorphous regions is thought to

be responsible for the initial crystallinity increase [83]. Poly(ethylene-tetrafluoroethylene) (ETFE/Tefzel), which is an isomer of PVDF as it also contains only CH_2 and CF_2 units, has similar radiation chemistry to PVDF and is widely used in nuclear power plants as cable insulation [84]. Since ETFE does not have a polar crystalline phase it does not display any piezoelectric effect.

Non-piezoelectric PVDF and copolymers of vinylidene fluoride with HFP, TrFE and chlorotrifluoroethylene (CTFE) were exposed to gamma-irradiation in vacuum up to doses of 1 MGy under identical conditions to obtain a ranking of radiation sensitivities. Changes in the tensile properties, crystalline melting points, heats of fusion, gel contents and solvent uptake factors were used as the defining parameters. The initial degree of crystallinity and film processing had the greatest influence on relative radiation damage, although the crosslinked network features were almost identical in their solvent swelling characteristics, regardless of the comonomer composition or content.

For commercial oriented PVDF homopolymer films the tensile properties varied greatly in the directions parallel and perpendicular to the fibril orientation. The tensile properties suffered rapidly after irradiation as a result of the orientation and would prevent use of these polymers in radiative environments while under stress. In the case of unoriented PVDF and copolymers, there were no significant differences in the effects of radiation on the elongation and stress at break. All materials can withstand radiation doses of at least 200 kGy before significant mechanical property changes develop. Irradiation caused a drop in the melting point of all polymers across the entire dose range studied and a general trend towards lower heat of fusion. Again, all polymers appeared to follow similar trends. The dose required for each polymer to reach an arbitrary soluble fraction (for example, $s + s^{1/2} = 1$) generally increased with initial crystallinity suggesting that chemical structure with this series of polymers is not as important as crystallinity. The exception was the CTFE copolymer (the only polymer in this study to contain chlorine) which appeared to have a higher affinity for chain scission. We can conclude that in terms of radiation induced changes, the oriented and unoriented PVDF homopolymers are the most sensitive, while the unoriented copolymers of HFP, TrFE and CTFE are more stable. The copolymers behaved similarly in terms of changes to the tensile properties but the degree of network formation was inversely proportional to the initial crystallinity with the exception of the CTFE copolymer, which despite low crystallinity, showed less crosslinking.

6. Overview of piezoactive films and optical quality considerations

The evaluation of piezoelectric PVDF in the space environment is just one aspect of the overall goal of making large-diameter thin film adaptive optics. In pursuit of this goal there are, of course, numerous engineering, modeling, mathematics and optics challenges to be addressed. Adding to this, we have also found there are several other materials issues which have arisen during the study of PVDF. These include the quality of the surface on the reflective side, the adhesive layer for bonding the piezoelectric films together, and the question as to how to fabricate very large films. In this section each of these points is briefly considered.

Currently, state-of-the-art mirrors, such as the James Web Telescope, use a lightweighted, structured geometry to optimize optical performance while yielding a higher stiffness-to-mass ratio. Most of these designs consist of a thin face and back sheet that encapsulates an inner honeycomb structure. Due to both the ease of material handling and polishing, and substrate stability, amorphous glass is the current material of choice for these structured mirrors. Because opticians also have a long legacy of working with glass, all of their tooling and techniques are designed to work with it. This traditionally results in an efficient production cycle with fewer unknowns during the fabrication process. Moving away from a

glass optical surface to a polymer surface may require a paradigm shift in processing techniques. Simply applying the glass polishing techniques to polymers may eliminate some of the macroscopic imperfections, but it does not address the fundamental issue of heterogeneity between the crystalline and amorphous makeup of semi-crystalline polymers such as PVDF, which will result in a surface with an intrinsic roughness on the nano-scale.

We have attempted to fabricate a PVDF laminate with a surface of optical quality by coating PVDF with a thin layer of a fully amorphous polyimide to "smooth out" the surface. The concept is presented in Fig. 24 and a photograph of an actual metallized polyimide on PVDF shown in Fig. 25. Polyimides are an obvious choice for the top coat as they can form smooth surfaces due to the highly aromatic planar structure causing chain alignment parallel to the surface. Similar results may also be achievable using curable polyurethanes or polybutadienes, which have been observed to form glossy finishes in other applications. The resistance to deformation by the coating should be minimized by using a low modulus material in a very thin layer.

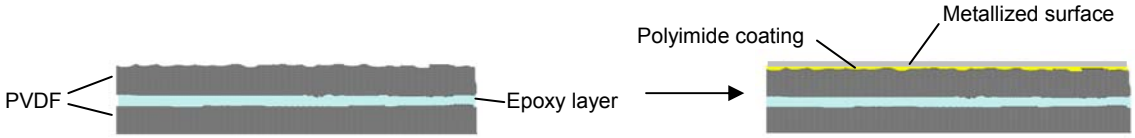

Figure 24. Schematic of a metallized PVDF bimorph

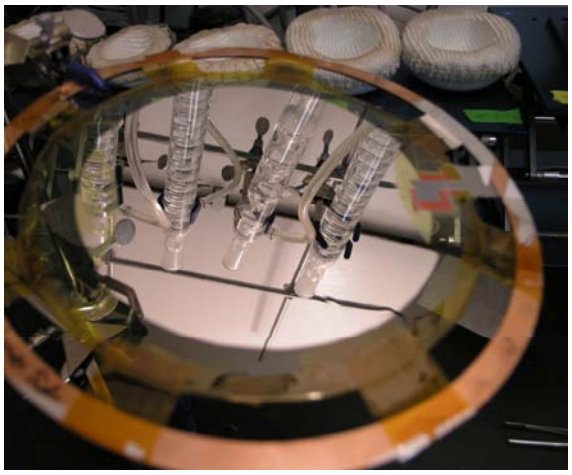

Figure 25. A photograph of a metallized polyimide on PVDF

To prepare a series type bimorph with one electrode on the top of the bimorph and one electrode on the bottom of the bimorph, the two piezoelectric layers must be bonded together with the piezoelectric polarity of each film in the opposite direction so that when the field is applied one layer expands and the other contracts. Alternatively, the parallel equivalent, which has a center electrode between the two layers in addition to the top and bottom electrodes, should be bonded with the polarity of each film in the same direction [85]. The adhesive layer should bond the films together sufficiently without causing any mechanical stiffening which will limit the total deflection during actuation. For epoxy adhesion, a general observation is that so long as the adhesive layer is kept thinner than 5 μm (for 30 μm piezoelectric films) there is no measurable loss in deformation. Interestingly, there appears to be no difference between using a glassy epoxy (Epon 828 cured with triethylene tetramine) with high modulus or a rubbery hydroxy terminated polybutadiene resin (cured with isophorone diisocyanate) with low modulus as the

adhesive layer below 5 μm. A potential problem with using multi-layered devices could be a mismatch in the coefficients of thermal expansion between the layers, which may cause unexpected warping. Even if the two piezoelectric layers of the bimorph are identical materials, there could still be an issue if they are oriented in a direction other than parallel to each other. This may result in shape distortion due to uneven expansion/contraction caused by temperature cycling. Such an effect would be magnified for larger films. This phenomenon is analogous to issues of stress relaxation and contraction as a function of temperature as discussed in section 5.2.

One other consideration which will become more important if larger prototype reflective films need to be fabricated, is how to process the PVDF into large diameter films. Other polymer film based space components, such as solar sails, have been built tens of meters in size by stitching smaller films together. This is an approach which may work for a thin film mirror, but if a seamless single piece is required then the ability to cast a large film becomes mandatory. Since the homopolymer requires stretching to obtain the polar β-phase it is not an attractive option for manufacturing of large films. The TrFE copolymer has the advantage that it spontaneously forms the β-phase without stretching and has slightly better solubility than the homopolymer, so that solvent casting into very large films is a definite possibility. So far this technique has been used to make 8-inch films by spin casting onto a silicon wafer and could easily be scaled up, the only limitation being the availability of a larger substrate and casting instrumentation.

7. Future work

7.1 Materials International Space Station Experiment (MISSE-6)

Until as recently as the 1980s very little was known about LEO environmental effects on polymeric materials. A significant step forward in the understanding of materials-space interactions and materials performance was based on retrieval and testing of materials from the Long Duration Exposure Facility (LDEF) Experiment which spent 69 months orbiting the Earth between 1984 and 1990. The LDEF experiment was a 14-sided passive satellite equipped with almost every type of spacecraft surface or material that was in use in the 1980s, or envisaged for potential use in the foreseeable future [3,5,11]. The LDEF mission demonstrated that all polymeric materials are greatly affected by the LEO environment with sometimes unexpected degradation occurring, that pre-LDEF knowledge of space environmental effects on materials had major flaws, and that synergistic effects of LEO environmental conditions must be considered to predict materials performance [3,5,11].

The LDEF mission spawned a number of subsequent smaller missions testing materials in the space environment aboard the Shuttle orbiter, Russian spacecrafts, and the International Space Station (ISS). Of these, only the Boeing/NASA experiments aboard the ISS (dubbed MISSE for Materials ISS Experiment) had any continuity with MISSE-1 through MISSE-5 having been launched, and MISSE-6 due for launch in early 2007 [86]. The MISSE program is designed to allow participation from government, academia and industry researchers, who require space testing of individual materials but may not have the multimillion-dollar budgets to host a launch. The participants in MISSE-6 are listed in Fig. 26.

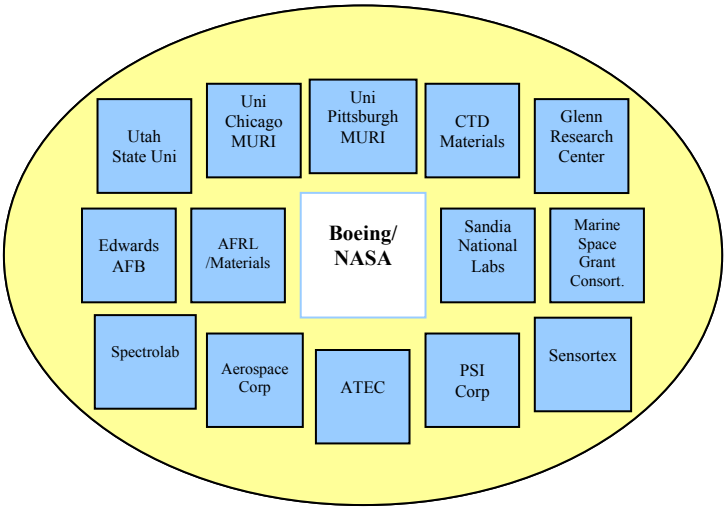

Figure 26. Participants in MISSE-6

Any use of novel responsive polymer components in space applications requires ground testing and ultimately space qualification to accommodate the complex LEO environment and understand materials degradation. SNL has been invited to contribute vinylidene fluoride piezoelectric samples to MISSE-6 offering an excellent opportunity to integrate the first flight experiment of piezoelectric polymers in LEO for space qualification. Since the materials are responsive there is also the opportunity to conduct active experiments, collect real-time data and evaluate the actual performance of these materials. This will be the first time that an active remote experiment has been part of the MISSE project. Both active and passive experiments will be flown allowing for a range of experiments and materials to be tested over the course of the exposure (estimated at 6-8 months, depending on the Shuttle flight program).

The MISSE experiments use a PEC (Passive Experiment Container) which is essentially a simple suitcase which houses the samples. The PEC is launched as a closed container where the samples are located on the inside, and is then attached to the ISS during a spacewalk (Fig. 27) and opened fully inside-out to expose the samples. Depending on which side of the PEC the samples are located, they will either receive primarily vacuum UV (VUV) radiation, or both VUV and atomic oxygen (AO) exposure. SNL has been allocated 6 x 6" on the VUV side and 6 x 4" on the AO/VUV side in which the passive and active experiments need to be located.

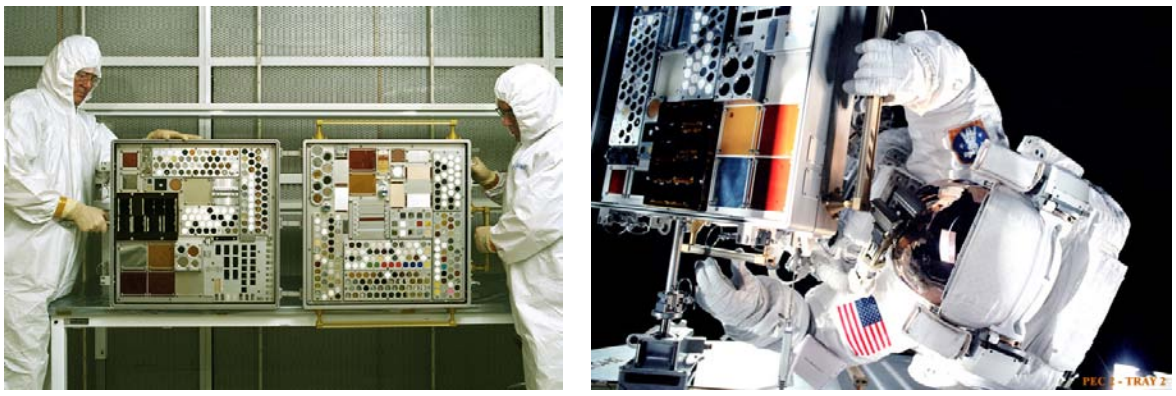

Figure 27. A MISSE PEC partially open **(left)**; installation of a PEC outside the ISS **(right)**

The passive experiments will use mounting fixtures similar to those used on previous MISSE missions to expose 30 μm and 100 μm films of the PVDF homopolymer and the 80:20 TrFE copolymer to both VUV and combined AO/VUV. Samples will have either no coating, or a gold or aluminum coating to examine the effects of metallization and may be either single films or multilayered bimporphs. Thin contact foil-type thermocouples will be used to measure the temperatures of the films. On return to Earth, the passive samples will be fully characterized to determine the effects of LEO. A summary of the passive samples to be flown is shown in Table 4.

Table 4. SNL samples for passive experiments on MISSE-6

AO/VUV side	VUV side
1" x 1" piezoelectric PVDF 30 μm thick from MSI USA Inc.	1" x 1" piezoelectric PVDF 30 μm thick from MSI USA Inc.
1" x 1" piezoelectric P(VDF_{80}-$TrFE_{20}$) 30 μm thick from Ktech Inc.	1" x 1" piezoelectric P(VDF_{80}-$TrFE_{20}$) 30 μm thick from Ktech Inc.
1" x 1" piezoelectric P(VDF_{80}-$TrFE_{20}$) 100 μm thick from Ktech Inc.	1" x 1" piezoelectric P(VDF_{80}-$TrFE_{20}$) 100 μm thick from Ktech Inc.
1" x 1" piezoelectric PVDF stack (2 x 30 μm thick with 1 μm epoxy layer in between) with Al coating (600 Å).	1" x 1" piezoelectric PVDF stack (2x 30 μm thick with 1um epoxy layer in between) with Al coating (600 Å).
	1" x 1" piezoelectric P(VDF_{80}-$TrFE_{20}$) stack (2 x 30 μm thick with 1 μm epoxy layer in between) with Al coating (600 Å).
	1" x 1" piezoelectric PVDF stack (2 x 30 μm thick with 1 μm epoxy layer in between) with Au coating (600 Å).
	1" x 1" piezoelectric PVDF 100μm thick from MSI USA Inc.
	1" x 1" piezoelectric P(VDF_{75}-$TrFE_{25}$) 30μm thick from Ktech Inc.

The active experiments were designed so that the performance of bimorphs made from piezoelectric PVDF or a TrFE copolymer mimicking small rectangular sections of a thin-film telescope mirror can be monitored in an actual LEO environment. A design was required that would allow for actuation of the bimorphs with relatively low voltage to produce a deflection large enough for detection with very simple and robust sensors. The chosen design relies on the bimorphs mounted at one end in a counter-lever configuration to give maximum deflection for a low actuation voltage. Under the tip of each bimorph is a LED/photodiode sensor, which can accurately measure a distance to the bimorph based on reflected IR light, with the analog sensor output being recorded using a data logger. The changes in the bimorph position (i.e. how much it will flex up or down with applied actuating voltage) over time will be used to determine relative changes in the piezoelectric responsiveness with LEO exposure. By also recording the temperature from the passive samples it will be possible to correlate the deflection properties with temperature conditions. The advantages of using the LED/photodiodes as opposed to a laser-type position sensor are that they have a larger temperature operating range, and are very robust and lightweight. The data loggers used will be NASA-qualified Veriteq-brand loggers designed for temperature and analog voltage input. The capacity of the data-loggers is limited to 70K 12-bit samples meaning they are not suitable for continuous position logging over the 6-9 months of the experiment. To obtain as much useful data as possible, measurements of the bimorph position and temperature (from the passive samples) will be made simultaneously three times every orbit plus 2 minutes, with the actuation voltage reversed every 24 hours, so that over time data will be available over the entire temperature cycling range (orbit dependent solar position). Four active bimorph experiments will be located on both the VUV and AO/VUV sides (Fig. 28). The materials for testing will be the PVDF homopolymer and the TrFE copolymer in various bimorph configurations. A list of the samples is presented in Table 5.

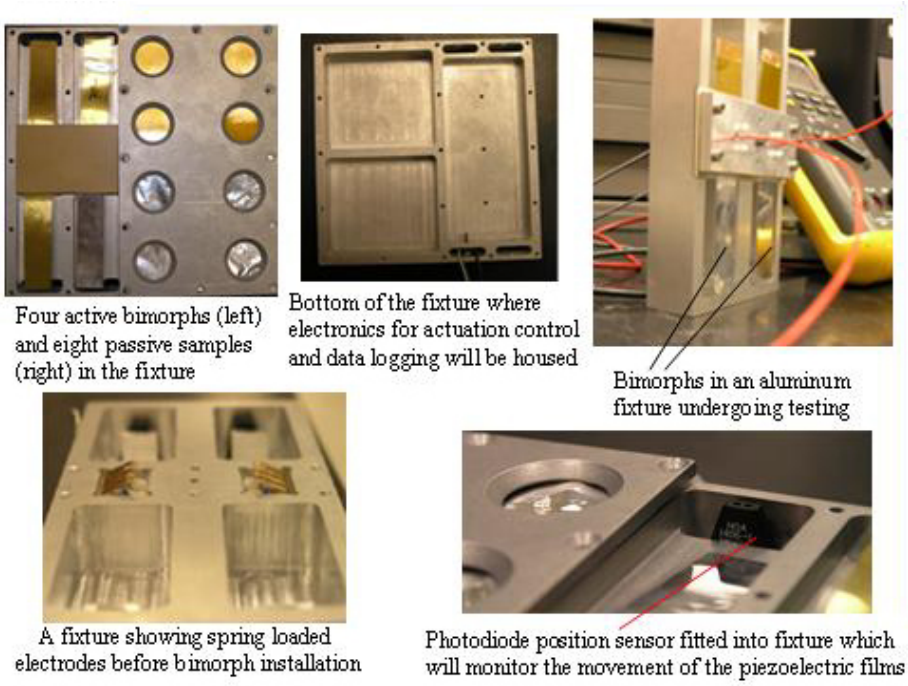

Figure 28. Photographs of the fixture housing active and passive samples for integration into the MISSE-6 base plate

Table 5. SNL samples for active experiments on MISSE-6

VUV and VUV/AO side
2.25" x 0.75" piezoelectric PVDF bimorph (2 x 30 μm thick with 1 μm epoxy layer in between) with aluminum coating (600 Å).
2.25" x 0.75" piezoelectric P(VDF_{80}-$TrFE_{20}$) bimorph (2 x 30 μm thick with 1 μm epoxy layer in between) with aluminum coating (600 Å).
2.25" x 0.75" piezoelectric P(VDF_{80}-$TrFE_{20}$) bimorph (2 x 100 μm thick with 1 μm epoxy layer in between) with aluminum coating (600 Å).
2.25" x 0.75" piezoelectric P(VDF_{80}-$TrFE_{20}$) bimorph (2 x 30 μm thick with 1 μm epoxy layer in between) with gold coating (600 Å).

Other than a power feed from the ISS, the experiments need to be self-sufficient. The sensors are regulated by components that are part of the data acquisition and control printed circuit board that was designed specifically to fit the bimorph mounting case and integrate all electronic features into a single unit. It consists of resistors to provide bias voltages and fuses to protect the sensors and external power supply source. A programmable (non-volatile memory) IC processor PIC 12C671 and 2 driver transistors provide the 24 hour clock pulse that will reverse the 100 volt bimorph excitation voltage via a miniature latching relay. All of these components are very low power consumption and are fuse protected as well. The PC board has a 15 pin D connector that provides the connections to the external 5 volt and 100 volt power supplies and four channels of analog voltage outputs (proportional to bimorph motion) to the external data loggers. The PC board is located inside the bimorph mounting unit where it will be shielded from direct solar irradiation, and to keep the wiring to the optical sensors and bimorph contacts as simple and compact as possible.

The electronics for driving and sensing the bimorphs are expected to receive a deeply penetrating radiation dose on the order of 50 krad (0.5 kGy) in LEO. This dose is far too low to cause any bulk

material damage, however, it may cause lattice displacement and other ionization effects, which can temporarily or permanently damage the electronics. The Veriteq data-loggers recently retrieved from MISSE-1 and -2 were found to be fully functional with no evidence of any data corruption, which is encouraging considering that they were not radiation hardened. For qualification purposes an optical sensor was exposed to 1 kGy (twice of what is expected in LEO) of γ-radiation and no negative effects on performance were observed, likewise we anticipate that when the PC board circuitry is exposed to radiation during ground testing it will remain operational.

The sensors work by measuring reflected light from an infrared LED adjacent to the photodiode and as such, are sensitive to stray light. In laboratory tests we found that a 'rolling' baseline was created from the stray light from an infrared lamp switched on and off at regular intervals to simulate passing in and out of the Earth's shadow. By subtracting the baseline it was possible to isolate the output from the sensor relating to the bimorph position. For the MISSE-6 active experiments it is anticipated that some stray light will impinge on the sensor. It should be possible to correct for these variations providing they are not too intense that it causes the sensor to go off-scale. To minimize any stray sunlight effects the sensors are located in the shadow of the bimorph with a window (slightly smaller than the bimorph) covering the sides of the bimorph. This window will reduce the exposure of the bimorph sides to the space environment, however may not completely eliminate any complications. In addition to the window, the trough below the bimorphs will be anodized resulting in a reduction of reflected light from the fixture onto the sensor.

The timetable for MISSE-6 is very strict as it revolves around the flight schedule of the Shuttle program. To date the experimental progress is on schedule within the Boeing/NASA project timetable. The experimental design and partial assembly has been completed, and the materials have been selected. Additional work including manufacturing of the electronic components and final assembly of the system and integration into the MISSE suitcase is still required.

7.2 Atomic oxygen resistance

In section 5.3 the potential for significant erosion of PVDF from atomic oxygen was demonstrated. Fortunately there are some methods for reducing the AO erosion yields using coatings or additives. Silica (SiO_2) is extremely resistant to AO erosion. If it is incorporated into a polymer, either as a coating or as part of the bulk material, erosion can be reduced. Coating a polymer with straight SiO_2 as an inorganic glass is not practical since all flexibility would be lost, so instead researchers at NASA Glenn have developed a SiO_x ($1.9 < x < 2.0$) filled PTFE which can be deposited as a film [8]. The method works by using a PTFE and a SiO_2 ion beam target to simultaneously sputter the two components onto the substrate. Compositions up to 16% PTFE by volume have been shown to exhibit high strain-to-failure, high transparency and AO durability. It is possible that such a coating would be suitable for PVDF, however, the thickness and composition of the coating would need to be optimized as to minimize the mechanical clamping effect while maximizing the AO protection.

An alternative method for introducing a protective SiO_2 layer can be achieved by the use of nano-sized particles of polyhedral oligomeric silsesquioxanes (POSS) dispersed into PVDF [87-89]. When exposed to AO, the POSS additive will react and form a self passivating, self healing silica layer protecting the underlying polymer. Preliminary experiments in collaboration with Edwards AFB in California have shown that incorporation of POSS into PVDF by blending is possible. Future work would require more detailed investigations on POSS interaction with the polymer and effects on the crystallite structure, Curie temperature, melting point, and piezoelectric properties. It is interesting to note that other workers have incorporated nanoparticles of silica or carbon nanotubes into a PVDF homopolymer and observed formation of the polar β-phase without stretching. If this were also to occur in POSS/PVDF composites it could lead to a novel unstretched version of a piezoelectric PVDF homopolymer with superior properties.

8. Summary and conclusions

This study has presented a comprehensive approach to establish selection criteria for PVDF and copolymers as adaptive materials in space applications. The most suitable avenues for polymer characterization were identified and the expected influence of LEO environments on materials performance explored. The complexity of LEO conditions was reviewed suggesting that the most important degradation pathways that will affect both physical and piezoelectric properties under these conditions are temperature, strong vacuum UV (radiation damage) and atomic oxygen exposure. Using LEO solar ultraviolet data, total UV energy depositions were estimated as equivalent radiation doses with significant doses on the order of many MGy's predicted for thin films. Out of various approaches for measuring piezoelectric properties, the two techniques of D-E hysteresis loops and direct d_{33} measurements were selected and used for monitoring degradative changes in accelerated aging studies.

Thermal exposure is a major reason for changes of piezoelectric properties and will lead to a new physical equilibrium of poled domains. This was concluded from the examination of various PVDF-based polymers in terms of temperature influence on the piezoelectric properties via d_{33} measurements and D-E hysteresis loops. Loss in d_{33} coefficients due to thermal annealing was attributed to randomization of the dipoles and consequentially loss of polarization. The stability of the polarization in decreasing order was: P(VDF_{80}-$TrFE_{20}$) copolymer>PVDF>P(VDF_{96}-HFP_4) copolymer. The remanent polarization (P_r) of the TrFE copolymer was more stable than the PVDF homopolymer over the range –80 °C to 110 °C which correlated with the deformation of bimorphs over a similar temperature range. Besides the limitations of other LEO environmental conditions these materials have the potential to operate at the temperatures anticipated in LEO (for example, if the thermal features of the design combined with thermal modeling would suggest temperatures below 100 °C). The reported upper use temperature of PVDF of 80 °C is overly conservative and the material retains residual but still useful piezoelectric properties at higher temperatures for extended periods of time. Unlike radiation damage, which may occur from vacuum UV and atomic oxygen in LEO, the depoling of the polymers on exposure to elevated temperatures was attributed to a physical randomization of the poled domains rather than a chemical degradation process.

Interestingly, good retention of piezoelectric properties during γ-irradiation was observed despite molecular level polymer damage with crosslinking, chain scission and morphological changes. A study directly comparing the radiation sensitivities under inert atmosphere of a large range of PVDF-based copolymers (including TrFE, HFP and CTFE comonomers) was performed to identify general trends and similarities relating to processing, comonomer type and content. For commercial oriented PVDF homopolymer films the tensile properties varied greatly in the directions parallel and perpendicular to the fibril orientation. The tensile properties suffered rapidly after irradiation as a result of the orientation and would prevent use of these polymers in radiative environments while under stress. In the case of unoriented PVDF and copolymers, there were no significant differences in the effects of radiation on the elongation and stress at break. All materials can withstand radiation doses of at least 200 kGy before significant mechanical property changes develop. We can conclude that in terms of radiation induced changes, the oriented and unoriented PVDF homopolymers were most sensitive, while the unoriented copolymers of HFP, TrFE and CTFE were more stable. The copolymers behaved similarly in terms of changes to the tensile properties but the degree of network formation was inversely proportional to the initial crystallinity with the exception of the CTFE copolymer which, despite low crystallinity, showed less crosslinking. It is important to emphasize, that the total radiation doses leading to significant changes in these material are beyond what would be expected in LEO conditions.

Atomic oxygen exposure resulted in significant erosive damage of thin films, but bulk properties in the remaining materials were retained. Detailed studies focused on the comparison the two most attractive

materials, the homopolymer and the P(VDF_{80}-$TrFE_{20}$) copolymer, and the effects of AO/VUV exposure on performance. In both cases significant weight loss and surface erosion resulted from AO attack. Erosion yields were $2.8x10^{-24}$ cm^3/atom for PVDF and $2.5x10^{-24}$ cm^3/atom for P(VDF-TrFE), consistent with previous literature data for similar materials. The film orientation of PVDF samples was reflected in the surface topology features after exposure, while the less orientated P(VDF-TrFE) samples had less regular surface patterning after exposure. The copolymer P(VDF-TrFE) showed a greater affinity for crosslinking due to the VUV radiation when compared with the PVDF homopolymer. Most importantly, the mechanical (tensile modulus) and piezoelectric properties in the remaining bulk material of both polymers were not significantly altered, while a decrease in the Curie transition of the copolymer resulted in poorer high temperature orientation of polar domains after exposure to AO/VUV.

In summary, these studies have resulted in a useful framework allowing for PVDF material selection, identified the critical performance criteria and established important qualification strategies for LEO applications of these polymers. Based on all the testing and experimental evaluations that could be conducted in a laboratory environment *it was concluded that the two most important materials, the PVDF homopolymer and the P(VDF_{80}-$TrFE_{20}$) copolymer, should perform satisfactorily under moderate LEO conditions*. As long as upper temperatures are limited to less than 110 °C and film thicknesses can accommodate some expected losses due to AO erosion, sufficient useful piezoelectric properties should remain and allow for remote actuation of bimorphs manufactured from these materials. Further qualification of selected polymers and multi-layer components utilizing these materials would have to be conducted as part of performance evaluations under actual space LEO environments. MISSE-6, the Materials International Space Station Experiment represents such an opportunity. A joint effort between Boeing, NASA and various materials research groups, it was possible to secure experimental space for the evaluation of active bimorph materials as part of a SNL contribution. The experimental design incorporating remote excitation, opto-electronic deformation measurements and periodic data-logging is the first ever attempt to evaluate the long-term performance of adaptive polymers in space, and was completed as part of this LDRD project. The experiment and components have been assessed as part of a Boeing/NASA primary design review and have been partially assembled. At the beginning of FY06 (printing of this document) final assembly and integration of the SNL experiment/contribution with the other MISSE components is dependent on additional internal funding.

9. Published papers and conference presentations

Further information and details on the experiments conducted as part of this project can be obtained in the open literature. All results and studies were summarized and published as unlimited release information.

Publications

1) **Piezoelectric PVDF materials performance and operation limits in space environments,** Celina, M. C., Dargaville, T. R., Chaplya, P. M., Clough, R. L., in *Materials for Space Applications,* edited by M. Chipara, D. L. Edwards, R. S. Benson, S. Phillips, *Material Research Society Symposium Proceedings.* **851** (2005) 449-460.

2) **Evaluation of piezoelectric PVDF polymers for use in space environments. Part I: Temperature limitations,** Dargaville, T. R., Celina, M., Chaplya, P. M., *Journal of Polymer Science, Part B Polymer Physics*, **43(11)** (2005) 1310-1320.

3) **Evaluation of piezoelectric PVDF polymers for use in space environments. Part II: Effect of atomic oxygen and vacuum UV,** Dargaville, T. R., Celina, M., Clough, R. L., Banks, B. A., *Journal of Polymer Science, Part B Polymer Physics*, **43(17)** (2005) 2503-2513.

4) **Selection and optimization of piezoelectric polyvinylidene fluoride polymers for adaptive optics in space environments,** Celina, M. C., Dargaville, T. R., Assink, R. A., Martin, J. W., *High Performance Polymers,* 2005, *in press.*

5) **Evaluation of vinylidene fluoride polymers for use in space environments: Comparison of radiation sensitivities,** Dargaville, T. R., Celina, M., Clough, R. L., *Radiation Physics and Chemistry,*2005, *in press.*

6) **Determining the crystallinity of polyvinylidene fluoride and copolymers**, Dargaville, T. R., Mowery, D. M., Assink, R. A., Tissot, R. G., Celina, M., *in preparation.*

7) **Evaluation of piezoelectric PVDF polymers for use in space environments. Part III: Comparison of the effects of vacuum UV and γ-radiation**, Dargaville, T. R., Skutnik-Elliott, J. M., Banks, B. A., Celina, M. *in preparation.*

Contributions to conferences

1) **Characterization, performance and optimization strategies for PVDF thin film piezo-electric materials,** M. Celina, J. Martin, R. Assink, P. Chaplya, S. Winters, R. Clough, *Fluorine in coatings conference V, 1/21-22/03, Orlando, FL.*

2) **Radiation and temperature induced limitations on the long-term piezoelectric properties of PVDF and copolymers,** M. Celina, T. Dargaville, P. Chaplya, J. Martin, R. Assink, R. Clough, *3rd International Symposium on Service Life Prediction, 2/1-2/6/04, Sedona, AZ.*

3) **Optimization of piezo-electric PVDF polymers for adaptive optics in space environments,** M. Celina, T. Dargaville, J. Martin, R. Clough, R. Assink, D. Mowery, *AIAA conference, 4/19-22/2004, Palm Springs, CA.*

4) **Evaluation of piezoelectric polymers for use in space environments,** T. Dargaville, M. Celina, R. Assink, P. Chaplya, *AIAA conference, 4/19-22/2004, Palm Springs, CA.*

5) **Optimization and characterization of piezoelectric PVDF polymers for adaptive optics in space environments,** M. Celina, T. Dargaville, J. Martin, R. Clough, R. Assink, D. Mowery, *National Space & Missile Materials Symposium, 6/21-6/25/2004, Seattle, WA.*

6) **Performance of piezoelectric PVDF copolymers for space applications,** Celina, M. C., Assink, R. A., Dargaville, T. R., Clough, R. L., *Fluoropolymers 2004, 10/7-10/9/2004, Savannah, GA.*

7) **Piezoelectric PVDF materials performance and operation limits in space environments,** M. Celina, T. Dargaville, R. Assink, R. Clough, Invited speaker *MRS Fall Meeting Symposium "Materials for Space Applications", 11/29-12/03/2004, Boston, MA.*

8) **Smart materials for gossamer spacecraft – performance limitations,** T. Dargaville, M. Celina, P. Chaplya, R. Assink, *46th AIAA Structures, Structural Dynamics, and Materials Conference, 4/18-21/2005, Austin, TX.*

9) **Optimization and characterization of piezoelectric PVDF polymers for adaptive optics in space environments,** M. Celina, T. Dargaville, J. Martin, R. Assink, R. Clough, *National Space & Missile Materials Symposium, 6/27-7/01/2005, Las Vegas, NV.*

10) **Piezoelectric vinylidene-fluoride based polymers for use in space environments**, T. R. Dargaville, M. Celina, R. L. Clough, *230th ACS Meeting, 8/28-9/1/2005, Washington, DC.*

10. References

[1] Berkey I. Advanced Space System Concepts and Technologies: 2010-2030+. California: The Aerospace Press, 2003.

[2] Martin JW, Redmond JM, Barney PS, Henson TD, Wehlburg JC, Main JA. Distributed Sensing and Shape Control of Piezoelectric Bimorph Mirrors. J Intel Mat Syst Str 2000;11:744.

[3] George PE, Dursch HW. Low Earth orbit effects on organic composites flown on the long duration exposure facility. J Adv Mater 1994;25:10.

[4] Young PR, Slemp WS. Space environmental effects on selected Long Duration Exposure Facility polymeric materials. ACS Symp Ser 1993;527:278.

[5] Young P, Siochi EJ, Slemp WS. Molecular-level response of selected polymeric materials to the low earth orbit environment. ACS Symp Ser 1996;620:264.

[6] Dever JA, de Groh KK, Banks BA, Townsend JA. Effects of radiation and thermal cycling on Teflon FEP. High Perform Polym 1999;11:123.

[7] Dever JA, de Groh KK, Banks BA, Townsend JA, Barth JL, Thomson S, Gregory T, Savage W. Environmental exposure conditions for Teflon fluorinated ethylene propylene on the Hubble space telescope. High Perform Polym 2000;12:125.

[8] Banks BA. In: Scheirs J, ed. Modern Fluoropolymers. Chichester: John Wiley & Sons, 1997. p 103.

[9] Clough RL, Gillen KT. In: Clegg DW, Collyer AA, eds. Irradiation Effects on Polymers. London: Elsevier, 1991. p 79.

[10] Dever JA, Bruckner J, Rodriquez E. Synergistic effects of ultraviolet radiation, thermal cycling, and atomic oxygen on altered and coated Kapton surfaces. NASA Tech Memo 1992-166134.

[11] Dursch HW, Pippin HG. In: Srinivasan V, Banks, B., ed. Materials Degradation in Low Earth Orbit (LEO). Warrendale: The Minerals, Metals & Materials Society, 1990. p 207.

[12] Hansen PA, Townsend JA, Yoshikawa Y, Castro JD, Triolo JJ, Peters WC. Degradation of Hubble space telescope metallized teflon FEP thermal control materials. 43rd Int. SAMPE Symp. 1998. p. 570.

[13] James BF, Norton OW, Alexander MB. NASA Reference Publication 1350, 1994.

[14] Silverman EM. 1995, NASA Contractor Report 4661.

[15] Pippin G. Spacecraft Materials Selector Expert System. http://see.msfc.nasa.gov/see/mp/model_sms.html, cited 16 March 2004.

[16] Seiler DA. In: Scheirs J, ed. Modern Fluoropolymers. Chichester: John Wiley & Sons, 1997. p 487.

[17] Cais RE, Kometani JM. New isomers of poly(vinyl fluoride) with controlled regiosequence microstructure. Polymer 1988;29:168.

[18] Lovinger AJ, Davis DD, Cais RE, Kometani JM. On the Curie temperature of poly(vinylidene fluoride). Macromolecules 1986;19:1491.

[19] Kepler GR. In: Nalwa HS, ed. Ferroelectric Polymers. New York: M. Dekkar, Inc., 1995.

[20] Lovinger AJ. Polymorphic transformations in ferroelectric copolymers of vinylidene fluoride induced by electron irradiation. Macromolecules 1985;18:910.

[21] Zhang QM, Bharti V, Zhao X. Giant electrostriction and relaxor ferroelectric behavior in electron-irradiated poly(vinylidene fluoride-trifluoroethylene) copolymer. Science 1998;280:2101.

[22] Cheng ZY, Olson D, Xu H, Xia F, Hundal JS, Zhang QM, Bateman FB, Kavarnos GJ, Ramotowski T. Structural changes and transitional behavior studied from both micro- and macroscale in the high-energy electron-irradiated poly(vinylidene fluoride-trifluoroethylene) copolymer. Macromolecules 2002;35:664.

[23] Bharti V, Xu HS, Shanthi G, Zhang QM, Liang K. Polarization and structural properties of high-energy electron irradiated poly(vinylidene fluoride-trifluoroethylene) copolymer films. J Appl Phys 2000;87:452.

[24] Mabboux P-Y, Gleason KK. ^{19}F NMR characterization of electron beam irradiated vinylidene fluoride-trifluoroethylene copolymers. J Fluorine Chem 2002;113:27.
[25] Buckley GS, Roland CM. Network structure in poly(vinylidene fluoride-trifluoroethylene) electrostrictive films. Appl Phys Let 2001;78:622.
[26] Kunstler W, Wegener M, Seiss M, Gerhard-Multhaupt R. Preparation and assessment of piezo- and pyroelectric poly(vinylidene fluoride-hexafluoropropylene) copolymer films. Appl Phys A: Mat Sci Proc 2001;73:641.
[27] Vinogradov A. In: Schwartz M, ed. Encyclopedia of Smart Materials. New York: John Wiley & Sons, Inc., 2002. p 780.
[28] Nalwa HS. Ferroelectric Polymers: Chemistry, Physics, and Applications. New York: M. Dekker Inc., 1995.
[29] Hesse J. PhD Thesis in Institute of Physics; University of Potsdam, 1999.
[30] Wegener M, Kunstler W, Richter K, Gerhard-Multhaupt R. Ferroelectric polarization in stretched piezo- and pyroelectric poly(vinylidene fluoride-hexafluoropropylene) copolymer films. J Appl Phys 2002;92:7442.
[31] Bauer F. PVF_2 polymers: ferroelectric polarization and piezoelectric properties under dynamic pressure and shock wave action. Ferroelectrics 1983;49:231.
[32] Harnischfeger P, Jungnickel BJ. Piezoelectric properties of electron-irradiated poly(vinylidene fluoride). Appl Phys A: Solid Surf 1990;A50:523.
[33] Simpson J, Ounaies Z, Fay C. Polarization and piezoelectric properties of a nitrile substituted polyimide. Mat Res Soc Symp Proc 1997;459:59.
[34] Ohigashi H. Electromechanical properties of polarized poly(vinylidene fluoride) films as studied by the piezoelectric resonance method. J Appl Phys 1976;47:949.
[35] Lee JW, Takase Y, Newman BA, Scheinbeim JI. Ferroelectric polarization switching in nylon-11. J Polym Sci Part B: Polym Phys 1991;29:273.
[36] Li G, Kagami N, Ohigashi H. The possibility of formation of large ferroelectric domains in a copolymer of vinylidene fluoride and trifluoroethylene. J Appl Phys 1992;72:1056.
[37] Newman BA, Scheinbeim JI, Lee JW, Takase Y. A new class of ferroelectric polymers, the odd-numbered nylons. Ferroelectrics 1992;127:1565.
[38] Su J, Ounaies Z, Harrison JS. Ferroelectric and piezoelectric properties of blends of poly(vinylidene fluoride-trifluoroethylene) and a graft elastomer. Mat Res Soc Symp Proc 2000;600:95.
[39] Hundal JS, Nath R. Piezoelectricity and polarization studies in unstretched SAN copolymer films. J Mater Sci 1999;34:5397.
[40] Giacometti JA, Ribeiro PA, Raposo M, Marat-Mendes JN, Campos JSC, DeReggi AS. Study of poling behavior of biaxially stretched poly(vinylidene fluoride) films using the constant-current corona triode. J Appl Phys 1995;78:5597.
[41] Hundal JS, Nath R. The piezoelectric effect and stored polarization in corona charged ABS films. J Phys D Appl Phys 1998;31:482.
[42] Dickens B, Balizer E, DeReggi AS, Roth SC. Hysteresis measurements of remanent polarization and coercive field in polymers. J Appl Phys 1992;72:4258.
[43] Ribeiro PA, Balogh DT, Giacometti JA. Corona poling and electroactivity in a side-chain methacrylate copolymer. IEEE T Dielec El In 2000;7:572.
[44] Tajitsu Y, Ishida M, Ishida K, Ohigashi H, Date M, Fukada E. Ferroelectric switching behavior in thin films of polyurea-5. Jpn J Appl Phys 2 1997;36:L791.
[45] Uchino K. Ferroelectric Devices. New York: Marcel Dekker Inc., 2000.
[46] Bar-Cohen Y, Sherrit S, Lih S-S. Characterization of the electromechanical properties of EAP materials. Proc SPIE - Int Soc Opt Eng 2001;4329:319.
[47] Mitrovic M, Carman GP, Straub FK. Durability properties of piezoelectric stack actuators under combined electro-mechanical loading. Proc SPIE - Int Soc Opt Eng 2000;3992:217.
[48] Scheirs J. Compositional and Failure Analysis of Polymers: A Practical Approach. Chichester: John Wiley & Sons, 2000.
[49] Brown R, ed. Handbook of Polymer Testing: Physical Methods. New York: Marcel Dekker, 1999.
[50] Celina M, George GA. Characterisation and degradation studies of peroxide and silane crosslinked polyethylene. Polym Degrad Stab 1995;48:297.
[51] Celina M, Gillen KT, Clough RL. Inverse temperature and annealing phenomena during degradation of crosslinked polyolefins. Polym Degrad Stab 1998;61:231.

[52] Nakagawa K, Ishida Y. Annealing effects in poly(vinylidene fluoride) as revealed by specific volume measurements, differential scanning calorimetry, and electron microscopy. J. Polym. Sci.: Polym. Phy. Ed. 1973;11:2153.
[53] Dargaville TR, Mowery DM, Assink RA, Tissot RG, Celina M. Determining the crystallinity of polyvinylidene fluoride and copolymers. in preparation 2005.
[54] Stidham CR, Banks BA, Stueber TJ, Dever JA, Rutledgem SK, Bruckner EJ. Low Earth orbital atomic oxygen environmental simulation facility for space materials evaluation. NASA Tech Memo 106128 1993.
[55] Kleiman JI, Iskanderova ZA, Gudimenko YI, Tennyson RC. Potential applications of hyperthermal atomic oxygen for treatment of materials and structures. Surf Interface Anal 1995;23:289.
[56] Navy. SUSIM: An NRL Program to Measure Solar Ultraviolet Irradiance. http://wwwsolar.nrl.navy.mil/susim.html, cited 16 March 2004.
[57] Floyd LE. SUSIM's 11-year observational record of the solar UV irradiance. Adv Space Res 2003;31:2111.
[58] Townsend JA, Hansen PA, Dever JA, Triolo JJ. Analysis of retrieved Hubble Space Telescope thermal control material. Sci Adv Mater Process Eng Ser 1998;43:582.
[59] Zuby TM, de Groh KK, Smith DC. Degradation of FEP thermal control materials returned from the Hubble Space Telescope. NASA Tech Memo 104627 1995.
[60] Dever JA, Townsend JA, Gaier JR, Jalics AI. Synchrotron VUV and soft X-ray radiation effects on aluminized teflon FEP. 43rd Int SAMPE Symp 1998. p. 616.
[61] Townsend JA, Hansen PA, Dever JA, Triolo JJ. Analysis of retrieved Hubble Space Telescope thermal control materials. Int SAMPE Symp Exhib 1998;43:582.
[62] Forsythe JS, Hill DJT. The radiation chemistry of fluoropolymers. Prog Polym Sci 2000;25:101.
[63] de Groh KK, Dever JA, Sutter JK, Gaier JR, Grummow JD, Scheiman DA, He C. Thermal contributions to the degradation of Teflon FEP on the Hubble Space Telescope. High Perform Polym 2001;13:401.
[64] Knowles GQ, Inc. http://research.hq.nasa.gov/code_s/nra/current/NRA-00-OSS-06/winners.html, cited 7 October 2005.
[65] Wang TT. Properties of piezoelectric poly(vinylidene fluoride) films irradiated by γ-rays. Ferroelectrics 1982;41:213.
[66] Jayasuriya AC, Schirokauer A, Scheinbeim JI. Crystal-structure dependence of electroactive properties in differently prepared poly(vinylidene fluoride/hexafluoropropylene) copolymer films. J Polym Sci Part B: Polym Phys 2001;39:2793.
[67] Tashiro K. In: Nalwa HS, ed. Ferroelectric Polymers. New York: M. Dekkar, Inc., 1995.
[68] Wang TT. Stress relaxation and its influence on piezoelectric retention characteristics of uniaxially stretched poly(vinylidene fluoride) films. J Appl Phys 1982;53:1828.
[69] Everett ML, Hoflund GB. Erosion study of poly(ethylene tetrafluoroethylene) (Tefzel) by hyperthermal atomic oxygen. Macromolecules 2004;37:6013.
[70] Gonzalez RI, Phillips SH, Hoflund GB. In Situ atomic oxygen erosion study of fluoropolymer films using X-ray photoelectron spectroscopy. J Appl Polym Sci 2004;92:1977.
[71] Kleiman JI, Gudimenko YI, Iskanderova ZA, Tennyson RC, Morison WD, McIntyre MS, Davidson R. Surface structure and properties of polymers irradiated with hyperthermal atomic oxygen. Surf Interface Anal 1995;23:335.
[72] Tuzzolino AJ, McKibben RB, Simpson JA, BenZvi S, Voss HD, Gursky H. The space dust (SPADUS) instrument aboard the Earth-orbiting ARGOS spacecraft: I-instrument description. Planet Space Sci 2001;49:689.
[73] Dargaville TR, Celina M, Chaplya PM. Evaluation of piezoelectric PVDF polymers for use in space environments. Part I: Temperature limitations. J Appl Polym Sci Part B: Polym Phys 2005;43:1310.
[74] Dargaville TR, George GA, Hill DJT, Whittaker AK. An investigation of the thermal and tensile properties of PFA following γ-radiolysis. Macromolecules 2003;36:7132.
[75] Clough RL, Gillen KT, Malone GM, Wallace JS. Color formation in irradiated polymers. Radiat Phys Chem 1996;48:583.
[76] French RH, Wheland RC, Qiu W, Lemon MF, Zhang E, Gordon J, Petrov V, Cherstkov VF, Delaygina NI. Novel hydrofluorocarbon polymers for use as pellicles in 157nm semiconductor photolithography: fundamentals of transparency. J Fluorine Chem 2003;122:63.
[77] Iezzi RA. In: Scheirs J, ed. Modern Fluoropolymers. Chichester: John Wiley & Sons, 1997. p 271.
[78] Banks BA, Snyder A, Miller SK, Demko R. Issues and consequences of atomic oxygen undercutting of protected polymers in low Earth orbit. NASA Tech Memo 2002-211577.
[79] Lyons BJ. Radiation crosslinking of fluoropolymers - a review. Radiat Phys Chem 1995;45:159.

[80] Florin RE, Wall LA. Gamma irradiation of fluorocarbon polymers. J Research Natl Bur Standards 1961;65A:375.
[81] Rosenberg Y, Siegmann A, Narkis M, Shkolnik S. Low dose γ-irradiation of some fluoropolymers: Effect of polymer chemical structure. J Appl Polym Sci 1992;45:783.
[82] Adem E, Rickards J, Burillo G, Avalos-Borja M. Changes in poly-vinylidene fluoride produced by electron irradiation. Radiat Phys Chem 1999;54:637.
[83] Zhao Z, Yu W, Chen X. Study on increase in crystallinity in γ-irradiated poly(vinylidene fluoride). Radiat Phys Chem 2002;65:173.
[84] Kerbow DL. In: Scheirs J, ed. Modern Fluoropolymers. Chichester: John Wiley & Sons, 1997. p 301.
[85] Piezoelectric transducers, TP-218. http://www.morganelectroceramics.com/pdfs/tp218.pdf, cited 7 October 2005.
[86] Materials International Space Station Experiment. http://misse1.larc.nasa.gov/, cited 7 July 2004.
[87] Gonzalez RI, Tomczak SJ, Minton TK, Brunsvold AL, Hoflund GB. Synthesis and atomic oxygen erosion testing of space-survivable POSS (polyhedral oligomeric silsesquioxane) polyimides. European Space Agency 2003;SP-540:113.
[88] Phillips SH, Haddad TS, Tomczak SJ. Developments in nanoscience: polyhedral oligomeric silsesquioxane (POSS)-polymers. Curr Opin Solid State Mat Sci 2004;8:21.
[89] Tomczak SJ, Marchant D, Svejda S, Minton TK, Brunsvold AL, Gouzman I, Grossman E, Schatz GC, Troya D, Sun L, Gonzalez RI. Properties and improved space survivability of POSS (polyhedral oligomeric silsesquioxane) polyimides. Mat Res Soc Symp Proc 2005;851:395.

Distribution

Unclassified Unlimited Release

2	MS-9018	Central Technical Files	8945-1
2	MS-0899	Technical Library	9616
1	MS-0161	Patent and Licensing Office	11500

1 Dr. Edward Stretanski
Ktech Corp. ABQ, Applied Physics and Testing Dept.
1300 Eubank Blvd. S.E., Albuquerque, NM 87123-3336

1	MS-0123	Donna L. Chavez, LDRD	1011
1	MS-0887	Duane B. Dimos	1800
1	MS-0885	Richard J. Salzbrenner	1820
3	MS-0888	Roger L. Clough	1821
5	MS-1411	Mathias C. Celina	1821
3	MS-1411	Tim R. Dargaville	1821
3	MS-0968	Jeffrey W. Martin	5714
2	MS-0972	Clinton A. Boye	5710
1	MS-0893	Pavel M. Chaplya	1523
1	MS-1310	Hartono Sumali	1524
1	MS-1360	David Baiocchi	5712
1	MS-1360	Todd J. Embree	5712
1	MS-0886	Gary D. Jones	1824
1	MS-1411	Julie M. Elliott	1821
1	MS-1411	Kenneth T. Gillen	1821
1	MS-0888	Robert Bernstein	1821
1	MS-1411	Roger A. Assink	1821
1	MS-1411	Daniel M. Mowery	1821
1	MS-1411	Ralph G. Tissot Jr.	1822
1	MS-1411	Bruce A. Tuttle	1816
1	MS-1415	Jonathan M. Campbell	1123